Dipole-induced effects on charge transfer and charge transport. Why do molecular electrets matter?

Journal:	*Canadian Journal of Chemistry*
Manuscript ID	cjc-2017-0389.R1
Manuscript Type:	Invited Review
Date Submitted by the Author:	09-Dec-2017
Complete List of Authors:	Derr, James; University of California, Riverside Tamayo, Jesse; University of California, Riverside Espinoza, Eli; University of California, Riverside Clark, John; University of California, Riverside Vullev, Valentine; University of California, Riverside,
Is the invited manuscript for consideration in a Special Issue?:	EDAI GRC
Keyword:	charge transfer, electron donors and acceptors, electric dipole, bioinspired, electrets

Dipole-induced effects on charge transfer and charge transport. Why do molecular electrets matter?

James B. Derr,[a] Jesse Tamayo,[b] Eli M. Espinoza,[b] John A. Clark,[c] Valentine I. Vullev[a,b,c,d,*]

[a] *Department of Biochemistry, University of California, Riverside, CA 92521, USA.*

[b] *Department of Chemistry, University of California, Riverside, CA 92521, USA.*

[c] *Department of Bioengineering, University of California, Riverside, CA 92521, USA.*

[d] *Materials Science and Engineering Program, University of California, Riverside, CA 92521, USA.*

* e-mail: vullev@ucr.edu ; Tel: (+1) 951-827-6239; FAX: (+1) 951-827-6416

Abstract. Charge transfer (CT) and charge transport (CTr) are at the core of life-sustaining biological processes, and of processes that govern the performance of electronic and energy-conversion devices. Electric fields are invaluable for guiding charge movement. Therefore, as electrostatic analogues of magnets, electrets have unexplored potential for generating local electric fields for accelerating desired CT processes and suppressing undesired ones. The notion about dipole-generated local fields affecting CT has evolved since the middle of the 20th century. In the 1990s, the first reports demonstrating the dipole effects on the kinetics of long-range electron transfer appeared. Concurrently, the development of molecular-level designs of electric junctions has led the exploration of dipole effects on CTr. Biomimetic molecular electrets, such as polypeptide helices, are often the dipole sources in CT systems. Conversely, surface-charge electrets and self-assembled monolayers of small polar conjugates are the preferred sources for modifying interfacial electric fields for controlling CTr. The multifaceted complexity of such effects on CT and CTr testifies for the challenges and the wealth of this field that still remains largely unexplored. This review outlines the basic concepts about dipole effects on CT and CTr, discusses their evolution, and provides accounts for their future developments and impacts.

Keywords: charge transfer, electron donors and acceptors, bioinspired, electric dipoles, electrets

1. Introduction

The importance of charge transfer (CT) and charge transport (CTr) for basic science and applied engineering cannot be overstated. The ability to control and guide charge transduction is of key importance for molecular and cell biology, for electronic design and development, and for energy science and engineering.[1-5] Electric fields, and in particular local fields originating from molecular dipoles and ordered ion pairs, offer an invaluable means for guiding CT and CTr. Due to dielectric asymmetry, for example, only a single CT pathway is favorable in the bacterial photosynthetic reaction center (RC), despite its pseudo C_2 structural symmetry, i.e., two-fold radial symmetry.[6-7] Furthermore, junctions containing such RC protein exhibit CTr rectification.[8] Conversely, electric fields in the vicinity of active sites of enzymes affect their catalytic activity.[9-12]

As systems with ordered electric dipoles, electrets present key structural motifs for introducing and modifying electric-field profiles along CT and CTr pathways.[13-16] Electrets however are inherently dielectrics. Reorganization of any free charge carriers would screen the dipole-generated fields and suppress their effects. Concurrently, the electrets of interest should mediate efficient CT and CTr to render themselves useful for electronic and energy-conversion applications.

Since the 1960s the idea about dipole effects on CT has gradually developed.[6-7, 17-19] In the late 1990s, the first reports providing direct experimental evidence about dipole-induced rectification of long range CT[20-22] commenced the development of the field and the growth of the interest in this phenomenon. For the last half a century, the focus has principally been on biological and biomimetic systems where polypeptide helices or polar groups in protein interior are the source of dipole-generated electric fields.[18, 20, 23-26] The first examples involving donor-bridge-acceptor (D-B-A) systems, where the bridges are a

polypeptide helices, illustrate a means for investigating CT kinetics for solution-based homogeneous conditions.[20] Employing self-assembled monolayers (SAMs) of polypeptide helices on conducting surfaces furthers the field to exploration of interfacial CT.[23] incorporating the similar helix SAMs in metal-insulator-metal (MIM) electrical junctions opens doors for bringing the field to CTr systems and device engineering.[27-28]

While protein helices encompass the best examples for molecular electrets, they do not mediate electron transfer efficiently along their backbones at distances exceeding 2 or 2.5 nm.[29-32] Another class of biopolymers, polynucleotides, which includes deoxyribonucleic acid (DNA) and ribonucleic acid (RNA) along with their biomimetic analogue peptide nucleic acid (PNA), readily mediate long-range CT along stacked aromatic moieties.[33-35] The charged backbones of DNA and RNA renders them unfeasible for electret designs. The non-charged PNAs have intrinsic dipoles and their strands,[36] if orderly stretched, can be viewed as molecular electrets. Hybridization into an antiparallel double helix, which improves the CT capabilities of PNAs, however, cancels the oppositely oriented dipoles from the two strands.

Accounting for the best features of biological electrets and biomolecular CT systems, we design bioinspired molecular electrets based on anthranilamide (Aa) motifs (Figure 1). Similar to protein helices, ordered amide bonds generate a macromolecular dipole. The hydrogen-bonding network not only supports the extended Aa conformation,[37] but also provides a polarization that enhances the total dipole of these molecular electrets (Figure 1a).[16] Unlike the protein helices, the aromatic Aa moieties and the extended π-conjugation along the Aa backbone provide pathways for efficient long-range CT (Figure 1b). These structures illustrate the unexplored potentials of bioinspired approaches to design and development of electronic and energy-conversion systems. Nature, indeed, presents great examples for mediating efficient CT and CTr. Taking ideas from the living systems and

employing them in an abiotic manner different from their biological counterparts, however, allows for attaining properties and characteristics that exceed what nature can offer.[38-45]

Herein, we review the basic concepts of CT and CTr and how they relate to dipole-induced effects. Description of the sources of molecular dipoles and local electric fields sets the foundation for elaborating the concept of molecular electrets and their utility for CT and CTr systems. The reported dipole effects on the CT focus on field-induced modification of the electrochemical potentials of the participating donor and acceptor, i.e., on the dipole-induced modulation of the CT driving forces, and hence, on the Franck-Condon contribution to the kinetics. When it comes to CTr molecular systems, involving MIM junctions, for example, the coupling between the molecule and the two electrodes can prevail the observed current-voltage (*I-V*) characteristics. In analogy with CT in donor-bridge-acceptor (D-B-A) conjugates, therefore, the effects of the dipoles on the molecular interfaces with the conducting substrates can most noticeably affect the *I-V* behavior of the junction, especially for off-resonance CTr regime. Overall, the D-B-A systems, incorporating molecular electrets, are excellent tools for discovery and understanding of structure-function relationships about dipole effects on CT, which proves important for furthering the basic science of electron donor-acceptor interactions. Concurrently, molecular and organic electrical CTr junctions, comprising electret films, provide some of the best paths for bringing this knowledge to the realms of applied science and engineering.

2. Basic concepts

Charge transfer (CT) encompasses a transition between two defined (electronic) states that have distinctly different charge distribution. As a subset of CT, electron transfer (ET) involves movement of negative charges, i.e., of electrons (e^-), while the changes in the nuclear geometry are small to negligible. Conversely, movement of the positively charged nuclei, such as protons (H^+), represents another type of CT, e.g., proton transfer (PT). To preserve electroneutrality, frequently PT and ET occur in a concerted step, i.e., as a proton-coupled electron transfer (PCET).[46-47] Photoexcitation that leads to opposite shifts in the pK_a characteristics of two neighboring protonatable sites can lead to excited state proton transfer (ESPT).[48-49]

ET occurs between an electron donor (D) and an electron acceptor (A). Transferring n electrons from a donor to an acceptor causes a positive shift in the charge of the donor and a negative shift in the charge of the acceptor:

$$D^x\text{-}A^y \rightarrow D^{x+n}\text{-}A^{y-n} \qquad \text{(ET)} \qquad (1a)$$

Where x and y are the charges of the donor and the acceptor, respectively, prior to ET. These changes in the charge states of the participating moieties make ET immensely susceptible to the local electric fields and to the solvating environment.

For successful ET, the reduction potential of the oxidation of the donor, $E_{D^{x+n}|D^x}^{(0)}$, should be smaller, i.e., more negative, than the reduction potential of the reduction of the acceptor, $E_{A^y|A^{y-n}}^{(0)}$. For the opposite case, i.e., when $E_{D^{x+n}|D^x}^{(0)} > E_{A^y|A^{y-n}}^{(0)}$, photoexcitation of the donor or the acceptor generates a locally excited (LE) state, analogous to an exciton, on the donor or the acceptor. This photoexcitation provides a means for initiating single-electron CT

(i.e., n = 1, eq. 1a) because the LE state of the donor oxidizes at a more negative reduction potential than its ground state; while the reduction of the LE state of the acceptor occurs at a more positive potential than its ground state. For such photoinduced electron transfer (PET) to be thermodynamically possible, the energy level of the highest occupied molecular orbital (HOMO) of the donor should be above that of the acceptor. Concurrently, the lowest unoccupied molecular orbital (LUMO) of the donor should also be above that of the acceptor.

$$D^{x}\text{-}A^{y} \rightarrow D^{x}\text{*-}A^{y} \rightarrow D^{x+1}\text{-}A^{y\text{-}1} \quad \text{(PET)} \quad \text{(1b)}$$

$$D^{x}\text{-}A^{y} \rightarrow D^{x}\text{-}A^{y}\text{*} \rightarrow D^{x+1}\text{-}A^{y\text{-}1} \quad \text{(PET)} \quad \text{(1c)}$$

The accepted convention for standard electrochemical potentials is to report them as *reduction potentials*.[50] Namely, $E^{(0)}_{A^y/A^{y-1}}$ represents the one-electron reduction of the acceptor, $A^y + e^- \rightarrow A^{y-1}$, and corresponds the energy level of its LUMO. For the donor, $E^{(0)}_{D^{x+1}/D^x}$ corresponds to the energy level of its HOMO, and represents the reduction of its oxidized form, $D^{x+1} + e^- \rightarrow D^x$. That is, $E^{(0)}_{D^{x+1}/D^x}$ is a reduction potential of the oxidation of the donor. The reduction and oxidation potentials of the same process can have opposite signs, depending on the reference.[51] This convention for using reduction potentials for representing electrochemical potentials causes two potential "confusions." (1) While the reduction potentials linearly relate to the energy levels of the frontier orbitals, this relationship has inverse proportionality. Lowering the energy levels of the orbitals makes the species better electron acceptors and easier to reduce. Hence, as the energies of the frontier orbitals become more negative, the reduction potentials become more positive.[50] (2) The broadly used designation of the electrochemical potentials places the oxidized over the reduced form, i.e., $E^{(0)}_{Ox/Red}$, which seems to represent the oxidation process of the redox couple, $Red \rightarrow Ox + e^-$. When adding, rather than subtracting, the logarithmic term in the Nernst equation for a half-

cell reaction, the activity of the oxidized form is in the numerator and the activity of the reduced form – in the denominator. Conversely, the convention for representing an electrochemical cell places the anode on the left and the cathode on the right side with the elections flowing from left to right through the external connectors. Therefore, for the cathode, along with the half-cell reduction, the oxidized species are on the left-hand side and the reduced – on the right, i.e., Ox|Red. Using slashes instead of vertical lines in the designations of electrochemical and electronic devices is not uncommon and it seems to validate the use of $E^{(0)}_{\mathrm{Ox/Red}}$ for reduction potentials. Strictly speaking, however, the reduction potentials should be represented as either $E^{(0)}_{\mathrm{Red/Ox}}$ or $E^{(0)}_{\mathrm{Ox|Red}}$.

Rehm-Weller equation provides a facile means for quantifying the driving force of PET, expressed as the negative of the change in the Gibbs free energy, $-\Delta G_{ET}^{(0)}$, in terms of experimentally measurable quantities:[52-53]

$$\Delta G_{ET}^{(0)} = F\left(E^{(0)}_{\mathrm{D}^{x+1}|\mathrm{D}^{x}} - E^{(0)}_{\mathrm{A}^{y}|\mathrm{A}^{y-1}}\right) - \mathsf{E}_{00} + \Delta G_S + W \qquad (2a)$$

Where E_{00} is the zero-to-zero energy, i.e., the excitation energy, of the donor or the acceptor; the Born solvation term, ΔG_S,[54] accounts for the variations in the solvation energy of the oxidized and reduced forms of the donor and the acceptor due to differences in the media for which the reduction potentials and E_{00} are estimated;[53] and W represents the donor-acceptor Coulomb interaction before and after PET.[55] For one-electron ET processes:[53]

$$\Delta G_S = \frac{q_e^2}{8\pi\varepsilon_0}\left(\frac{2x+1}{r_{\mathrm{D}}}\left(\frac{1}{\varepsilon}-\frac{1}{\varepsilon_{\mathrm{D}}}\right) - \frac{2y-1}{r_{\mathrm{A}}}\left(\frac{1}{\varepsilon}-\frac{1}{\varepsilon_{\mathrm{A}}}\right)\right) \qquad (2b)$$

Where q_e is the electron charge; x and y are charge of the donor and the acceptor (eq. 1); r_D and r_A are the effective radii of the donor and the acceptor, respectively;[56] ε_D and ε_A are the relative dielectric constants of the media for which the reduction potential of the donor and the acceptor, respectively, are recorded; and ε_0 is the dielectric constant of the media for PET and for which $\mathfrak{S}_{00}$ is estimated.

$$W = \frac{(y - x - 1)q_e^2}{4\pi\varepsilon_0\varepsilon R_{DA}} \quad (2c)$$

Where R_{DA} is the center-to-center distance between the donor and the acceptor.

The Rehm-Weller equation provides thermodynamic considerations. It allows for testing if the photoinduced CT processes are possible and what the energy losses for the transition from the LE to CT states are. For evaluating the efficiency of CT and how it competes with other processes occurring in parallel, it is essential to resort to kinetic analysis. Marcus transition state theory provides a means for evaluating the rate constants, k_{ET}, of ET:[57]

$$k_{ET} = \frac{4\pi^2}{h}\left|H_{if}\right|^2 \mathrm{FCWD}\left(\Delta G_{ET}^{(0)}, \lambda\right) \quad (3a)$$

Where the coupling between the initial (ground or LE) state and the final (CT) state, H_{if}, represents the donor-acceptor electronic coupling; the Franck-Condon weighted density of states (FCWD), i.e., the nuclear contribution to the kinetics, accounts for the overlap and density of vibrational states at the transition state; and h is the Planck constant, introducing the fundamental frequency. Prior knowledge of the driving force and the reorganization energy, λ, allows for estimating FCWD. For non-adiabatic processes, Marcus-Hush formalism represents eq. 3a as an Arrhenius-type expression in terms of the transition-state

energy, $\Delta G^{\dagger}$, where FCWD $\propto \exp(-\Delta G^{\dagger} / k_B T)$ and $\Delta G^{\dagger} = (\Delta G_{ET}^{(0)} + \lambda)^2 / 4\lambda$, k_B is the Boltzmann constant, T is the temperature, and $k_B T$, thus, is the thermal energy:[58-59]

$$k_{ET} = \frac{4\pi^2}{h} \left| H_{if} \right|^2 \frac{1}{\sqrt{4\pi\lambda k_B T}} e^{-\frac{\left(\Delta G_{ET}^{(0)} + \lambda\right)^2}{4\lambda k_B T}} \qquad (3b)$$

For certain non-adiabatic systems, eq. 3b tends to underestimate k_{ET}.[60-61] The Gaussian expression for FCWD($\Delta G_{ET}^{(0)}$, λ) in eq. 3b accounts for the distribution of only low-frequency modes, the energy levels of which are close enough to one another to allow for treating them as a quasi-continuum density of states. To address this classical limitation, Jortner introduced high-frequency modes to FCWD, which requires the consideration of quantum-mechanical nuclear tunneling. Substantial contributions of such tunneling to the ET kinetics lead to larger values of k_{ET} than what eq. 3b can yield. The semi-classical Marcus-Levich-Jortner formalism expands the FCWD factor in terms of the ET driving force, the reorganization energy, and a high-energy vibrational frequency, ν_C, important for the CT process:[7, 62-63]

$$k_{ET} = \frac{4\pi^2}{h} \left| H_{if} \right|^2 \frac{e^{-S_C}}{\sqrt{4\pi\lambda k_B T}} \sum_{j=0}^{\infty} \frac{S_C^j}{j!} e^{-\frac{\left(\Delta G_{ET}^{(0)} + \lambda_m + jh\nu_C\right)^2}{4\lambda k_B T}} \qquad (3c)$$

Where λ_m is the media, or outer-sphere, reorganization energy, i.e., $\lambda_m = \gamma\,((2r_D)^{-1} + (2r_A)^{-1} - R_{DA}^{-1})\, q_e^2\, (4\pi\varepsilon_0)^{-1}$ and γ accounts for the Born solvation energy originating from the orientational, $\mathbf{P}_{\mu}$, and vibrational/nuclear, $\mathbf{P}_{\nu}$, polarization of the solvent, $\gamma = (n^{-2} - \varepsilon^{-1})$;[64-65] S_C is the Huang-Rhys factor, $S_C = \lambda_i\, (h\nu_C)^{-1}$; λ_i is the inner-sphere reorganization energy; and

the frequency ν_C represents either a single vibrational mode, or be an average of the frequencies of several modes. While this single-mode semi-classical model (eq. 3c) accounts only for one high frequency, its relative simplicity makes it an important tool for analysis of ET processes.

Considering that the lifetimes of LE states of good photosensitizers are between sub-nano to microseconds, k_{ET} should be at least 10^6 s^{-1}, and ideally exceed 10^{10} s^{-1}, for attaining efficient photoinduced CT. It places limits on the feasible range of non-adiabatic CT since H_{if} tends to decrease exponentially with the donor-acceptor distances.

When the donor and the acceptor are not charged, i.e., $x = y = 0$, ET leads to charge separation (CS). That is, an electron moves from the donor to the acceptor leaving a positive charge, i.e., a hole (h^+), behind. ET, or PET specifically, leads to separating a positive from a negative charge:

$$D\text{-}A \rightarrow D^{\bullet+}\text{-}A^{\bullet-} \quad \text{(CS)} \quad (4a)$$

$$D\text{-}A \rightarrow D^{*}\text{-}A \rightarrow D^{\bullet+}\text{-}A^{\bullet-} \quad \text{(photoinduced CS)} \quad (4b)$$

$$D\text{-}A \rightarrow D\text{-}A^{*} \rightarrow D^{\bullet+}\text{-}A^{\bullet-} \quad \text{(photoinduced CS)} \quad (4c)$$

Photoinduced CS (eq. 4b,c) is referred to as *exciton dissociation* in solid-state physics. Charge recombination (CR) encompasses the back ET that brings the CT state to the ground state:

$$D^{\bullet+}\text{-}A^{\bullet-} \rightarrow D\text{-}A \quad \text{(CR)} \quad (4d)$$

The concept of charge separation is not limited to non-charged donors and acceptors.[60, 66-67] ET leads to a positive shift in the charge of the donor and negative shift in

the charge of the acceptor (eq. 1). Regardless the initial changes of the CT moieties, during PET the LE state or the exciton dissociates to place an electron on the acceptor and a hole (i.e., a positive charge) on the donor (eq. 1b,c). Therefore, PET leads to separation of the charges composing the excitons, that is, to CS.

At a supramolecular and mesoscopic scales, CS can take on a different connotation. For bulkheterojunction (BHJ) media, for example, a CS state comprises an electron and a hole that are sufficiently separated and/or energetically rich to prevent attractive interactions,[68] i.e., the emphasis is on "separation" in the term "charge separation." Conversely, a CT state in BHJ is Coulombically trapped at the interface between the donor and the acceptor media and can undergo efficient CR.[69-70]

When the donor and/or the acceptor are singly charged, CS can shift or completely remove their charges, which presents interesting sets of CT cases. If the donor is negatively charged or the acceptor is positively charged, ET leads to charge shift (CSh).[71] Specifically, when CS places a positive charge on a donor that has a single negative charge, the donor becomes non-charged. Similarly, CS converts a positively charged acceptor into a non-charged moiety. When CS eliminates the charge of a donor or an acceptor, while placing a charge on a non-charged acceptor or donor, respectively, the net result is CSh, i.e., a shift of the positive charge of the acceptor to the donor (for $x = 0$ and $y = 1$, eq. 1), or of the negative charge of the donor to the acceptor (for $x = -1$ and $y = 0$, eq. 1):

$D^{-}\text{-}A \rightarrow D^{\bullet}\text{-}A^{-}$ (CSh) (5a)

$D\text{-}A^{+} \rightarrow D^{+}\text{-}A^{\bullet}$ (CSh) (5b)

$D^{-}\text{-}A \rightarrow (D^{-})^{*}\text{-}A \rightarrow D^{\bullet}\text{-}A^{-}$ (photoinduced CSh) (5c)

$D^{-}\text{-}A \rightarrow D^{-}\text{-}A^{*} \rightarrow D^{\bullet}\text{-}A^{-}$ (photoinduced CSh) (5d)

$D\text{-}A^{+} \rightarrow D^{*}\text{-}A^{+} \rightarrow D^{+}\text{-}A^{\bullet}$ (photoinduced CSh) (5e)

$D\text{-}A^{+} \rightarrow D\text{-}(A^{+})^{*} \rightarrow D^{+}\text{-}A^{\bullet}$ (photoinduced CSh) (5f)

A special case encompasses CT systems with negatively charged donor (such as phenolate, x = -1) and positively charged acceptor (such as acridinium, y = 1) where CS leads to eliminating of the charges of both the donor and the acceptor. That is, CS, involving ET from the donor to the acceptor, causes charge annihilation (CA) leading to a non-charged CT state:

$D^{-}\text{-}A^{+} \rightarrow D^{\bullet}\text{-}A^{\bullet}$ (CA) (5g)

$D^{-}\text{-}A^{+} \rightarrow (D^{-})^{*}\text{-}A^{+} \rightarrow D^{\bullet}\text{-}A^{\bullet}$ (photoinduced CA) (5h)

$D^{-}\text{-}A^{+} \rightarrow D^{-}\text{-}(A^{+})^{*} \rightarrow D^{\bullet}\text{-}A^{\bullet}$ (photoinduced CA) (5i)

CA differs from CR (eq. 4d). While CA leads to a CT state, CR involves a transition from a CT to the ground state.

The strict requirement for electroneutrality, however, places a question of what CSh processes truly are. The definition of CSh and CA is based on the charge states of the donor and the acceptor before and after ET. Charged species, however, cannot exist free without counterions around them, especially when in non-polar media. Therefore, CSh processes moving a positive charge from the acceptor to the donor (eq. 5e,f) technically lead to CS of the positive charge from the counter-anions next to the acceptor. Similarly, CSh from a negatively charged donor (eq. 5c,d) results in CS of the negative charge from the counter-cations in the vicinity the donor. Furthermore, considering the presence of counterions makes it quite reasonable to classify CA as CS (eq. 4d), i.e., the annihilation of the charges of the donor and the acceptor leaves counter-cations around the donor and counter-anions around the acceptor. This view of CSh and CA as CS when considering all charges around the CT

conjugates is especially pronounced for viscous media that impedes the migration of ions and makes the reorganization of their distribution considerably slower than the ET processes. Indeed, a consequent movement of the counterions to preserve the electroneutrality contributes to the reorganization energy and dynamics, affecting the kinetics of CT.

Are there truly genuine CSh processes? After all, the first experimental demonstration of the Marcus inverted region utilized CSh kinetics.[72-74] Indeed, starting with non-charged CT conjugates always helps. The first step, however, requires charging one of the moieties of such non-charged conjugates. That is, oxidizing the acceptor or reducing the donor initiates ET from the donor to the acceptor and shifts of the generated charge within the CT conjugate. The initial generation of the charge on the donor or the acceptor, however, generates also a counter charge next to it. If the counter-charge species are unstable, decompose and dissipate away fast enough, they leave a singly charged donor-acceptor conjugate to undergo CSh. If the counter-charge lingers, the CSh becomes CS. Arbitrarily, therefore, when most studies refer to CSh, they focus on the shift of positive or negative charges solely within the donor-acceptor conjugates.

While considering counterions and solvation may blur the definitions of CS, CSh and CA, the local fields within and around the solvation cavities of the donor and the acceptor profoundly affect the CT dynamics. That is, the kinetics of CSh involving CT between charged and non-charged moieties (eq. 5a-f), differs from the CS kinetics between non-charged donors and acceptors (eq. 4a-c). Despite the electroneutrality, the field gradients in the vicinity of solvated non-charged moieties and of charge moieties with their counterions are profoundly different. For example, the higher frequency of the solvent phonons around charged moieties, in comparison with that around non-charged donors and acceptors, strongly affects the CT dynamics.[75] Adding permanent dipoles to the donor-acceptor conjugates in

order to modulate the profiles of the local electric fields sets an important multifaceted paradigm for controlling CT dynamics that still remains largely unexplored.

Solvatochromism provides a potential means for discerning CS from CSh should the donor-acceptor conjugates exhibit CT absorption and emission bands. Regardless the charge states of donor and the acceptor, CS changes the dipole moments of the CT conjugates. The Onsager solvation energy of dipolar species,[76] therefore, governs the relaxation upon the transitions: (1) from the Franck-Condon excited state to the CT state, and (2) from the Franck-Condon ground state (after radiative deactivation from the CT state) to the ground state minimum. Stokes' shift, $\Delta\tilde{\nu}$, between the LE absorption and the CT emission, thus, corresponds to the change in the dipole moment resultant from CS. As depicted by the Lippert-Mataga-Ooshika formalism, $\Delta\tilde{\nu}$ is linearly proportional to the Onsager polarity function, $\Delta f_O(\varepsilon, n^2)$, and the slope quantifies the difference between the electric dipole moments of the ground and the excited state, $\Delta\mu$:[77-79]

$$\Delta\tilde{\nu} = \frac{\Delta\mu^2}{hcR^3}\Delta f_O\left(\varepsilon, n^2\right) + \Delta\tilde{\nu}_0 \qquad (6)$$

Where R is the radius of the donor-acceptor conjugate, h is the Planck constant, c is the speed of light, $\Delta f_O(\varepsilon,n^2) = f_O(\varepsilon) - f_O(n^2)$, where $f_O(\text{ж}) = 2(\text{ж} - 1)/(2\,\text{ж} + 1)$, and $\Delta\tilde{\nu}_0$ is the Stokes' shift for a non-polar medium with $\Delta f_O(\varepsilon,n^2) = 0$. The Onsager solvation function $\Delta f_O(\varepsilon,n^2)$ eliminates the contribution of the electronic polarization of the solvent, $f_O(n^2)$, from the total one, $f_O(\varepsilon)$; thus, $\Delta f_O(\varepsilon,n^2)$ depicts the solvation due to the orientational and vibrational modes of the media. While the Lippert-Mataga-Ooshika formalism has proven beneficial for analysis of CS processes,[80-81] it is based on several key assumptions: (1) the dipoles of the ground and the CT state have the same orientation; (2) the donor-acceptor conjugate is in a

spherical solvation cavity with a radius *R* (eq. 6); (3) the contributions from the polarizability of the solvated conjugate is negligible; and (4) the solvent is a continuum with a bulk refractive index, *n*, and a static dielectric constant, ε, and its molecular-level interactions with the solvated species are negligible.

On the other hand, CSh involves a movement of a charge (or of a charge and a counterion). If CSh causes a minimum dperturbation in the dipole moment of the donor-acceptor conjugate, Born solvation energy, which depends inversely on the size of the ion,[54] should dominate the stabilization or the destabilization of the CT excited state. For example, if CT involves a shift of a positive charge from a small acceptor to a large donor, or of a negative charge from a small donor to a large acceptor, the energies of the ground and the LE state will be more sensitive to solvent polarity than the energy of the CT state. For such cases, polar medium stabilizes the ground and the LE state more than the CT state. Therefore, an increase in solvent polarity causes hypsochromic shifts in the CT absorption and emission without significantly perturbing the LE spectral bands.[71] Conversely, the CT spectral shifts will be bathochromic when CSh involves transfer of electron or hole from a larger to smaller moieties. When the donor and the acceptor have a similar size, the CT bands will manifest negligible solvatochromism. Overall, employing general solvation models, such as the Born-Kirkwood-Onsager ones,[82] for the analysis of solvatochromism and solvatofluorochromism of CT absorption and emission offers a promising potential for determining the CS vs. the CSh character of ET processes.

The initial PET step is of upmost importance for conversion of light into electrical energy. A means for attaining long-range CT, i.e., driving the photogenerated charge carriers a few nanometers away from the location of the LE state, proves significant. While increasing the distance between the donor and the acceptor increases the distance of PET, it also decreases the strength of the electronic coupling between them and decreases the rates of CT.

The distance dependence of the CT kinetics strongly depends on the bridging media between the donor and the acceptor. If in a donor-bridge-acceptor (D-B-A) system, the electron directly tunnels from the donor to the acceptor, the CT rates decrease exponentially with distance. Indeed, such a superexchange mechanism involving e^- tunneling along virtual states of the bridge has inherent length limitations for its efficiency (Figure 2a).

Bridging media that can host charges and provides pathways for a sequence of short but efficient tunneling steps allows for overcoming the distance limitations for long-range CT. For example, bridging units, with their LUMOs below the LUMO of the donor and above the LUMO of the acceptor, provide pathways for long-range CT via *electron hopping* (Figure 2c). That is, the LE donor reduces the bridging moiety next to it, injecting an electron in its LUMO. The electron migrates along the LUMOs of the other bridge components until it reaches the acceptor. Conversely, a bridge with HOMOs below the HOMO of the donor but above the HOMO of the acceptor, can mediate long-range CT via *hole hopping* following the photoexcitation of the acceptor (Figure 2d). The LE acceptor can extract an electron from a neighboring bridge moiety to generate a vacancy or hole, h^+, on it. Another electron from a different bridge residue moves to the vacancy, and thus h^+ moves further away from the reduced acceptor. After a series of such ET steps along the HOMOs of electron-rich bridge units, the hole reaches the donor. That is, in such hole hopping, an electron from the donor does not physically move to the acceptor.

Overall, the process involves a series of short shifts of electrons between HOMOs of the D-B-A system that results in a long-range hole transfer (HT). In analogy, a single-step CT, involving electron tunneling from the HOMO of a donor to the HOMO of LE acceptor, is occasionally referred to as *hole tunneling* and hole transfer (Figure 2b). Long-range CT occurring via electron or hole hopping involves initial CS followed by a sequence of CSh steps.

The rates of CT occurring via electron hopping or hole hopping have negligible distance dependence. Therefore, such incoherent mechanism involving hopping provides a superb efficiency for long-range CT, exceeding a few nanometers, in comparison with a single concerted tunneling or superexchange ET step.

Charge transfer, CT, involves transitions between well-defined single states. Conversely, transitions of electrons or holes between media with multiple states, such as conductors and semiconductors, are representative of charge transport (CTr). In biology, ion transport is another type of CTr that is crucially important for vitality of cells.[83-84] Similar to the bridge in a D-B-A system, the media between two metallic or semiconductor surfaces can provide pathways for electron tunneling (Figure 3a). Such CTr mechanism encompasses *off-resonance* electron transport or hole transport depending if it involves transitions from the conduction or the valence bands, respectively.[85] In contrast, *on-resonance* CTr involves electron or hole hopping along sites in the media connecting the conducting or semiconducting surfaces (Figure 3b,c). While rate constants and $-\Delta G^{(0)}$ are features of CT processes, electrical currents and potentials are a principal means for characterizing CTr.

The different types of CT lead to either generating charges or changing the position of charges in D-A and D-B-A conjugates. The orientation or the magnitude of the dipole moments of the CT states is different from that of the LE and the ground states. Therefore, electric fields affect the rates of CT mediated by D-A pairs or by D-B-A conjugates. Stark effects, attributed to Johannes Stark,[86-87] reflect the manner in which external electric fields affect the electronic and spectral properties of molecular systems, encompassing effects on the CT characteristics of D-A and D-B-A samples.[88] Unless controlled using self-assembly, the orientation of the CT conjugates in such samples is random, making it challenging to interpret spectral Stark-effect data.[88]

Local electric fields, originating from dipoles with fixed orientations in relation to the CT systems, offer an attractive alternative. Constructs with permanent dipole moments, which are components of D-B-A systems, provide an excellent means for introducing local electric fields and shaping them in accordance with the needed direction of CT. That is, such dipolar conjugates allow for exploring Stark effects at a molecular and nanometer scales.

How do electric fields affect the rates of CT? An electric field oriented along the axis connecting the donor and the acceptor alters the difference between their reduction potentials, changing the ET driving force, $-\Delta G_{ET}^{(0)}$ (eq. 2a). A permanent electric dipole pointing from the donor to the acceptor stabilizes the CT state, increasing $-\Delta G^{(0)}$ of CS and decreasing $-\Delta G^{(0)}$ of CR (eq. 4). Thus, such a dipole orientation increases the rates of CS and CR, if CS is in the Marcus normal region and the CR in the inverted region. A dipole oriented from the acceptor to the donor exerts an opposite effect. The direction of an electric dipole is from its negative to its positive pole.[89] This field effect on the CT driving force, i.e., on the nuclear or the Franck-Condon component of the CT kinetics (eq. 3), encompasses the most widely accepted notion of how dipoles affect ET.[21, 90]

As evident from observed Stark effects on vibrational transitions,[91-92] electric dipoles, and the local fields they generate, have the potential to affect the reorganization energy for CT processes. Although unexplored, such field effects on the reorganization energy offer an alternative means for modifying the Franck-Condon component of CT kinetics.

In addition to the Franck-Condon considerations, the CT kinetics strongly depends on the electronic coupling between the donor and acceptor, i.e., on how well the LE or the ground state is coupled with the CT state. Field-induced changes in the electron distribution of the frontier orbitals can alter the donor-acceptor electronic coupling. This field effect reveals the manner in which dipoles can affect the electronic component of the CT kinetics.

Separate exploration of the different dipole effects on individual aspects of the CT rates is, indeed, plausible via careful design of D-A and D-B-A systems. Synergy between the different aspects of dipole effects on the CT kinetics, however, presents promising and immensely attractive ways for controlling CT and optimization of CT systems. As we demonstrated, dipole effects on the nuclear component of the CT kinetics tend to be prevalent for processes with relatively small driving forces, such as CS.[61] Conversely, for CT processes with relatively large $-\Delta G^{(0)}$, such as CR, the donor-acceptor electronic coupling dominates over the effects on the nuclear component of the kinetics.[61]

For CTr through dielectric media, the dipole effects are analogous to those for CT. Dipolar molecules on the surfaces of a semiconductor affects its ionization energy.[93-94] For molecular species placed between two electrodes, asymmetries in coupling with the two conducting surfaces can exert dominating effects on the performance of such junctions frequently seen as rectification behavior in their *I-V* curves. The *I-V* curves show the variations in current in response to applied voltage to the device termini; and rectification, *R*, represents differences in the absolute magnitude of the current when reversing the polarity of the voltage, i.e., $R = \lg(|I(V)| / |I(-V)|)$. Therefore, non-zero *R* indicates for a preferred directionality of the transport of the charge carriers. Indeed, the design and development of heterogeneous multi-scale systems, with incorporated dipole-generated local electric fields for controlling CTr, have immediate practical implications. Conversely, exploration of dipole effects on CT mediated in D-A and D-B-A conjugates, frequently introduced in solution-phase as homogeneous samples, including in viscous and solid solvents,[95-98] provides a means for discovery, understanding and unequivocal characterization of new phenomena and structure-function relationships. That is, while studies on CT are key for advancing the field and the fundamental knowledge of dipole-induced phenomena, transferring this knowledge to CTr provides crucial routes for pushing the frontiers of electronic and energy engineering.

3. Sources of dipoles for controlling charge transfer

Structural asymmetry that leads to separating the centers of the positive and negative charges results in electric dipole moments. Indeed, the nuclear geometry defines the center of the positive charges, and the electron density distribution – the center of the negative charges. The amount of charge displaced from each other and the distance of the displacement determines the magnitude of dipoles, quantified as charge times distance or Debyes (D), i.e., 1 D ≈ 0.208 e Å ≈ 3.34 × 10^{-30} C m. While the dipole magnitude is a scalar, the dipole moment itself is a vector quantity showing the direction of the charge displacement. Despite some discrepancies in the physics and chemistry literature, the direction of electric dipoles is from the negative to the positive center of charges.[89]

Introducing dipoles in CT systems can be as simple as preferential adsorption of ions,[99] and as complex as multi-scale assemblies of elaborate three-dimensional structures with well-defined orientation of polar groups.[100] In the organic and bioorganic molecular realm, many conjugates tend to be polar. After all, living systems are based on low symmetry and high entropy. Polar molecules intrinsically have dipole moments. Dipole moments are characteristic for the simplest of molecules such as hydrofluoric acid, and for some of the biologically-originated complex structures such as protein helices.[101-103]

Strength of dipoles depend on the electronegativity of the atoms, on the bonding patterns between them, and on their spatial arrangement. Polar functional groups, attached to non-polar molecular species provide some of the simplest means for introducing molecular dipoles to CT systems and exploring the effects of the fields they generate.[104-105] Self-assembled monolayers (SAMs) of alkyls terminated with dipolar moieties modulate the electronic and interfacial CT properties of materials and devices. Changes in the work

function of metal conductors coated with such dipole-containing SAMs is one of the most apparent effects.[106] The flexibility of the alkyl termini in the SAMs, however, can prevent co-directional packing of the polar groups due to dipole-dipole interactions.[107] Large polar moieties that pack well, such as perfluorinated segments of the alkyl chain, can address this issue.[106, 108] SAMs of rigid molecular moieties, in which the polar groups attached to them or incorporated in them with fixed directions, provide attractive alternatives.[109-111] Many of these rigid structures are linked aromatics with extended π-conjugation.

Small aromatic molecules with electron-donating or electron-withdrawing groups are invaluable for modulating materials properties without compromising the efficiency of interfacial CT. The functional groups polarize aromatic rings making them electron rich or electron deficient. Such polarization produces electric dipoles. For example, placing an amine on a phenyl results in a molecular dipole of about 3 D, and a nitro group – in a dipole of about 4 D with opposite orientation.[93-94] Employing such small dipolar derivatives as surface ligands alter the electronic properties of quantum dots (QDs). Electric dipoles pointing toward the surface of a QD (the positive pole of the dipole pointing toward a chalcogenide QD when using 4-nitrothiophenol, for example) increases its ionization energy, i.e., lowers the energy of the quantum confined bands of the nanomaterial.[93-94] Conversely, ligands with electric dipoles pointing away from the QD surface, such as 4-aminothiophenol attached to CdSe, lifts the energy levels of the QD frontier orbitals / confined bands, as reveled by the shifts in the QD electrochemical reduction potentials.[93] Indeed, the extent of this dipole effect depends on the packing density of the orientation of the surface ligands, and on the size and the chemical composition of the QDs. Examples with CdSe nanomaterials show shifts of 0.5 eV in the energy levels of the QD bands when the dipole of the small aromatic ligands varies over 4.6 D.[93] Similarly, varying the molecular dipoles of the aromatic ligands over 6.2 D, causes 0.7-eV shift in the energy of the valence band (VB) of PbS QDs.[94] As an alternative,

temporal dipoles from excited-state polarization, involving small organic ligands on QD surfaces, also affects CT kinetics and device performance.[112]

The surface dipoles appear to have a small effect on the bandgap of the nanomaterials.[94] It is not clear if this effect results from differences induced by the dipoles on the valence and conduction bands of the QDs, or differences in electronic conjugation with the coating ligands. The electron-donating and withdrawing functional groups have different balance between the inductive and mesomeric effects on the aromatic rings. Therefore, difference in long-range electronic coupling between the QD orbitals and the electron-donating and withdrawing groups attached to the distal positions of the aromatic rings can affect the bandgaps of the semiconducting material. Specifically, narrowing of the QD bandgap when the functional group on the ligand changes from methyl to nitro illustrates improved stabilization of VB in comparison with the conduction band (CB).[94]

Pairing electron donors and acceptors, by bridging them with π-conjugated systems, forms push-pull class of compounds.[113] Retinal activation during the photodetection occurring in our eyes, utilizes such push-pull configuration.[114] Improvement of photovoltaic (PV) devices can benefit from employing push-pull strategies. The push-pull geometry yields in a dipole moment facilitating the preference in the directionality of ET or HT event. For electron donors and acceptors, usually, push-pull macromolecules comprise electron-donating and electron-withdrawing groups, such as amines and nitro groups, respectively, attached to opposite sides of aromatic or other π-conjugated system. Varying the electron donating and withdrawing strengths of these groups results in ground-state permanent dipole moments readily exceeding 5 D.[115] These dipoles point from the electron-withdrawing to the electron-donating groups. Push-pull complexes can, indeed, affect HT and ET kinetics when incorporated in CT pathways. Aligning the push-pull dipoles with the direction of CT accelerates it or slows it down depending on their orientation, i.e., leading to CT rectification.

Zwitterionic π-conjugates derivatives present another important class of compounds that can provide permanent dipole moments for controlling charge transfer and charge transport.[100] Such zwitterions are a subclass of push-pull complexes where the positively charge moieties act as an electron-withdrawing acceptors, and the negatively charged ones as donors. Junctions containing such zwitterioninc species manifest rectifying characteristics.[100] A principal challenge with using charged species to define field effects on CT is the dynamics of the counterions that can be potentially present. While a zwitterion does not require counterions, they are inherent components of compounds with a net-positive or net-negative charge. Indeed, free ions can readily rearrange to screen the permanent dipoles and diminish their effects on CT kinetics. Furthermore, the motility of counterions affects the reorganization energy and the Franck-Condon component of the CT kinetics.

4. Electrets and macromolecular dipoles

Small polar molecules and ion pairs can feasibly provide permanent electric dipoles of a few Debyes. Assembling polar moieties provide a means for achieving dipoles that can considerably exceed 10 D. Such assemblies have additive effect on the resultant total dipole. For example, the total dipole of a stack of polar groups oriented in the same direction is the sum of the dipoles of the comprising moieties (Figure 4). Separated charge, q, times the distance of the separation, d, quantifies the magnitude of a dipole:

$$\mu = q\ d \qquad (7a)$$

In a stacked geometry of identical polar groups, each with a dipole of $\mu_i = q_i\ d_i$, the total distance of charge separation, d, is equal to that of the individual comprising dipoles, i.e., $d =$

d_i. In such assembly, however, each polar group adds to the total amount of separated charge, i.e., $q = \Sigma_i\, q_i$. Therefore, the total dipole of the stacked assembly is the sum of the dipoles of the comprising polar moieties (Figure 4b), i.e.,

$$\mu = d\, \Sigma_i\, q_i = \Sigma_i\, \mu_i \qquad (7b)$$

For assemblies of polar moieties arranged in a head-to-tail manner, the charge at the positive pole of one dipole cancels with the negative charge of the neighboring one (Figure 4c). As a result only two terminal charges remain uncompensated. Hence, the total amount of charge separated is the same as the charge displaced in each individual building block, i.e., $q = q_i$. Conversely, the distance between the terminal charges of such tightly assembled head-to-tail constructs, is the sum of the charge displacement in each individual polar moiety, i.e., $d = \Sigma_i\, d_i$. Therefore, the magnitude total dipole of this type assembly is also an additive quantity of the dipoles of the individual groups, i.e.,

$$\mu = q\, \Sigma_i\, d_i = \Sigma_i\, \mu_i \qquad (7c)$$

Indeed, stacked and head-to-tail assemblies of dipoles represent two extreme cases. They, however, illustrate the additive nature of the total intrinsic dipole moments of any assembly of polar groups. The vector sum of the dipoles of the comprising components represents the total dipole of any assembly, i.e.,

$$\boldsymbol{\mu} = \Sigma_i\, \boldsymbol{\mu}_i \qquad (7d)$$

In analogy with magnets, **electrets** are such systems comprising ordered electric dipole moments. Oriented-dipole electrets refer to the assemblies of polar groups (Figures 1a, 4b and 4c). Conversely, (real-)charge electrets encompass ions or other charged moieties (1) assembled as layers on surfaces, generating dipoles across the interface, forming surface-charge electrets, or (2) displaced in the bulk of dielectric materials, forming space-charge electrets. To avoid the challenges with the motility of free ions and counterions, non-charged electrets, i.e., oriented-dipole electrets, present the preferred alternative for CT systems.

Biology offers some of the best examples for macromolecular electrets. As molecular electrets, protein α-helices have intrinsic dipole moments that amount to 5 D per residue originating from co-directional orientation of the peptide bonds, i.e., the amides connecting the neighboring residues, as well as of the hydrogen bonds, keeping the secondary structure intact.

The magnitude and direction of protein dipoles was not confidently determined until the advent of X-ray crystallography. The dipole of a protein depends on three components: (1) the fixed surface charges, (2) the core polar residues mainly the amide bonds, and (3) the fluctuation of proton movement.[116]

In protein α-helices, each amide bond contributes about 3.4 – 3.7 D to the total dipole. The polarization due to hydrogen bonding points from the hydrogens to the oxygens, which is consistent with the negatively charged electron pair shifting toward the hydrogen. Hence, each hydrogen bond connecting neighboring helix loops adds about 1.5 – 1.7 D to the total dipole,[117] resulting in a total of about 5.2 D per amino acid.[90] For example, the dipole from four amino acids in a peptide α-helix, i.e., from a single turn, amounts to about 20 D. Other helical secondary structures of native α-L-amino acids also possess substantial intrinsic dipole moments.[90] Similar to the α-helix, the tightly folded conformer, 3_{10}-helix, has a dipole of 4.6 D per residue.[90] The nomenclature 3_{10} indicates three residues per a turn with 10 bonds

making the complete loop between two neighboring hydrogen bonds connecting the turns. In fact, the α-helix is 3.6_{13}-helix. The polyprolines, however, do not have a hydrogen-bonding network because they only comprise tertiary amides along their backbone. Change in the peptide bonds in polyprolines from *E* to *Z*, can change the type of helical conformation and flips the direction of the total intrinsic dipole, i.e., polyproline type I (PPI) has a dipole of -4.1 D per residue, and type II (PPII) – of 1.5 D per residue or less.[90] The other most abundant secondary structure of proteins, β-sheets, does not possess a considerable electric dipole, i.e., 0.25 D per residue, because the configuration of the amide and hydrogen bonds causes their dipoles to cancel out, i.e., the sum of the vectors of the comprising dipoles (eq. 7d) is close to zero.

In the PPI structure, the amide carbonyls are parallel to the helix axis with their oxygens oriented toward the N-terminus. It results in the large PPI dipole pointing from the N- to the C-terminus.[118] In the PPII secondary structure, on the other hand, the carbonyls are almost perpendicular to the helix axis, resulting in a relatively small total dipole. A slight tilt in the amide bonds, however, can switch the direction of the helix dipole, which reflects the opposing reports on this electronic feature of PPII.[90, 118]

While protein helices are excellent sources for molecular dipoles, their backbones do not efficiently mediate long-range ET or HT. Conversely, the π-stacked electron-rich nucleobases in DNA double helices provide excellent pathways for long-range HT.[33-34] The negatively charged phosphates in DNA backbones, along with the surrounding counter cations render these polymers impractical for electret designs. Conversely, peptide nucleic acid (PNA) oligomers and polymers are structurally similar to DNA biomacromolecules, forming double helices that can efficiently mediate HT.[33, 119] Unlike DNAs, however, PNAs have an electrically neutral polypeptide backbone. The peptide bonds, i.e., the amides, in the PNA backbone produce intrinsic dipole in extended single-strand PNAs.[36] Similar to

polypeptide α- and 3_{10}-helices, the dipole of PNAs is orientated from their C- to their N-termini. The conformational flexibility of single-stranded PNAs compromises the electronic coupling between the bases and the CT pathway. Conversely, the double-stranded PNAs are limited to parallel, rather than antiparallel, configuration to avoid dipole cancelation.

Based on features of the different dipolar biological and biomimetic macromolecules, and of biopolymers that mediate long-range CT, we develop bioinspired molecular CT electrets that are polypeptides composed of non-native aromatic β-amino acids, i.e., derivatives of anthranilic acid (Figure 1a).[120-126] Anthranilamide molecular electrets possess intrinsic dipoles, which in similarity with protein helices, originate from ordered arrangement of amide and hydrogen bonds (Figure 1a).[15-16, 38, 61] Similar to DNAs and PNAs, these bioinspired electrets contain closely positioned aromatic moieties that can provide pathways for long-range CT (Figure 1b). The hydrogen-bonding network, along with and the preferred *Z* conformation of the amides, ensures an extended secondary structure, stretching at about 0.45 nm per residue. Furthermore, the polarization resultant from the formation of the hydrogen bonds causes cumulative shift of electron density from the oxygens to the hydrogens and enhances the molecular dipole. Thus, each hydrogen bond contributes about 1 D to the total dipole, while each amide – about 2 D. The extended π-conjugation along the backbone of the anthranilamides provides not only pathways for CT, but also certain rigidity of the structure.

Each of the aromatic moieties can serve as a site where charges can reside for mediating long-range charge transfer via electron or hole hopping; as well as charge transport via on-resonance mechanism. The two side chains on the anthranilamide residues (R_1 and R_2, Figure 1a) serve a key role for (1) controlling solubility and propensity for self-assembly of the molecular electrets, and (2) adjusting the electronic and photonic properties of CT electrets. For example, electron-withdrawing or electron-donating side chains make the

residues electron-deficient or electron-rich, respectively, to promote ET or HT.[16] Extending the π-conjugation over the side chains narrows the HOMO-LUMO energy gap, i.e., the bandgap of the electrets. Balancing between the inductive and mesomeric effect of R_1 and R_2 substituents on the aromatic rings provides a means for decoupling the control over the energy-level of the electret residues and over the distribution of the density of the frontier π-orbitals.[123] Overall, the anthranilamide motif provides the extended π-conjugated structure with intrinsic permanent electric dipole, and the side chains allow for flexibility in the electronic and CT properties of these bioinspired molecular electrets.

5. Dipole effect on long-range charge transfer

Since the late 1950s, the idea about dipole effects on CT has gradually evolved through the second half of the 20th century.[7, 17-19] It was in the late 1990s, however, when Galoppini and Fox reported the first experimental evidence about dipole-induced rectification of long-range CT.[20-22] Using a biomimetic D-B-A construct, in which the bridge is a synthetic helical polypeptide, they demonstrated that the CT rates can be more than an order of magnitude larger when the ET direction is along the helix dipole rather than against it.[20-22] The biomimetic design introduces the electron donor and acceptor as side chains of non-native L-alanine derivatives, six residues apart (i.e., about two helical loops) in the middle of 14-mer polypeptides. Comparison between two basic constructs, with the acceptor closer to the C-terminus than the donor and vice versa, provides the best means for testing the dependence of the ET kinetics in comparison with the helix macrodipole. Photoexcitation of the acceptor induces a single-step ET from the HOMO of the donor via tunneling along the

polypeptide backbone. Strictly speaking, this CT process is a HT, i.e., via superexchange along virtual states energetically close to the HOMOs of the amide bonds.

The CT rectification, i.e., the difference between the rates of ET along vs. against the dipole, shows dependence on solvent polarity.[20-21, 61] While an increase in solvent polarity usually stabilizes the CT state and accelerates CS leading to it (eq. 4a-c), polar solvents screen the dipole generated-field and diminish its effect. Ultimately, the use of aqueous electrolyte solution as a media completely eradicates the effect of the helical dipole on CT.[127]

The dependence of the CT rectification on solvent polarity appears straightforward considering the screening of the dipole-generated field. While it is the correct way of thinking, an increase in media polarity tends to enhance the dipole strength. A molecular dipole polarizes the solvation media around it. Aligning the solution and ion-pair dipoles, as much as allowed by the entropic limitations, moves the centers of the positive and negative charges further apart from each other, hence, increasing the magnitude of the dipole (eq. 7c). That is, the total amount of displaced charge is still the same, but the distance of displacement increases (eq. 7c). This induced polarization, referred as formation of image charges in electrical engineering and solid-state physics, enhances the electric field inside the solvation cavity, i.e., generates an Onsager field.[65, 76] That is, while an increase in media polarity suppresses the dipole-generated field outside the solvation cavity, it enhances the field within the cavity. This feature reveals an important strategy for enhancing the dipole effects on CT. For many designs, electron donors and acceptors are attached via flexible linkers to the peptide helices, which are the macromolecular dipole sources. Thus, the donors, the acceptors and the macromolecular dipoles are in separate solvation cavities. Only the dipole field that is external to its cavity can affect the properties of the donor and the acceptor and have an effect on the CT kinetics (Figure 5a,b). The evanescent components of the wave functions of the donor and the acceptor, indeed, extend and overlap inside the solvation cavity of the

macromolecular dipole source. Unless the dipole drastically affects the polarization of these evanescent parts of the wave functions and their overlap depends on its orientation, the internal cavity field would have negligible to no effect on the CT kinetics. Conversely, designs involving incoherent e^- or h^+ hopping, or on-resonance CTr, such as molecular electrets based on anthranilamides (Figure 1a), permit the transferred charges to spend a relatively long time inside the solvation cavity (Figure 5c,d). That is, the ordered amide and hydrogen bonds responsible for the total dipole and the aromatic moieties mediating each individual CSh step are in the same solvation cavity (Figure 1b), allowing for dramatic additive effects on the long range CT and CTr (Figure 5b,c). For such molecular geometries, using the media polarity to balance the enhancement of the dipole field inside the solvation cavity with suppression of the field extending outside, presents unexplored means for contriving CT and CTr.

Following the first work from Galoppini and Fox,[20-22] about every five years new sets of publications testify for waves of renascence of the interest in dipole effects on long-range CT.[23, 90] With a few exceptions, all reports on this subject utilize polypeptide helices as sources for the macrodipoles. Detailed analysis reveals that all protein helical structures composed of α-L-amino acids possess substantial dipole moments aligned with the principal axis of the helices; and it affects differently $-\Delta G_{ET}^{(0)}$ of ET along or against it.[90] Among these secondary structures, the dipole moment was greatest for the α-, 3_{10}-, and PPI helices. The dipole of the PPI conformers, however, is small and can be oriented in the same or opposite direction to that of α and 3_{10} ones.[90, 118] While the dipole affects the FC component of the ET kinetics by changing the driving force (eq. 2, 3), the assumed macromolecular secondary structure affects the donor-acceptor electronic coupling, H_{if}. In addition, because of the lack of primary of secondary amides, the polyproline helices, PPI and PPII, do not offer inter-turn tunneling pathways for ET via hydrogen bonds. The hydrogen-bonding network in the other

helical structures can prove crucial for the CT kinetics.[128-130] An increase in the distance between the donor and the acceptor increases the dipole-induced changes in $-\Delta G_{ET}^{(0)}$ because it increases not only the magnitude of the CS dipole, but also the difference between the electric potential that the helix dipole exerts on the donor and on the acceptor.[90] An increase in the donor-acceptor distance, however, decreases H_{if}, and causes an exponential decrease in k_{ET}. Therefore, balancing the distance dependence of H_{if} and the dipole effect on the FC components of the ET kinetics is essential in the design of polypeptide systems for rectifying CT.

Designed fullerene-peptide-radical non-charged constructs show that the helix dipoles shift the reduction potentials of the donor and acceptor, and modify the rates of long-range CT.[131] Employing a radical cation as an acceptor with a relay of two donors on PPII scaffolds allows for examining the effect of dipoles on two-step CSh.[24, 132-133] The use of charged constructs involving counterions, along with the relatively small dipole of PPII, makes the interpretation of the CT results somewhat challenging. Placing the non-native α-L-amino acids with redox-active side chains three prolines apart, i.e., on neighboring turns, allows for attaining CT via hole-hopping mechanism.[24, 132-133] Conversely, placing redox active species on α-helices, as side chains of residues, one or two-turns apart from one another, does not aid CT and CTr.[134-135] For example, CTr through assembly of polypeptide helices with and without ferrocene in the side chains of some of the residues show the same *I-V* characteristics, indicating for off-resonance CTr involving tunneling pathways along the macromolecular backbone.[134] These reports illustrate the importance of the electronic coupling in defining the pathways of long-range CT in macromolecular systems.

Similar to alkylthiols, polypeptide helices derivatized with sulfhydryl or thioether moieties at one of their termini form well packed self-assembled monolayers (SAMs) on surfaces of coinage metals.[136] Kimura utilizes such SAMs of α-helices to demonstrate the

dipole effect on interfacial CT between a gold electrode and liquid media.[23] Such liquid junctions, comprising SAMs of ordered helix dipoles, rectify photocurrents.[23] Using electrochemical analysis of such electrodes modified with SAMs of α-helices allows for detecting extremely slow CT processes with rate constants as small as 1 s^{-1}.[137] In addition to polypeptide α-helices, SAMs of oligoprolines on metal electrodes manifest similar dipole-induced rectification of interfacial CT.[138]

Some suggested mechanisms for long-range CT along the backbones of polypeptides of native α-L-amino acids encompass charge hopping. Electrochemistry of aliphatic amides, however, reveals that they oxidize irreversibly,[139] i.e., placing a positive charge on a peptide bond, needed for accommodating hole hopping, leads to oxidative degradation. This instability of oxidized amides renders CT via charge hopping along polypeptide backbones highly impractical and implausible.

The use of polypeptides allows for exploring functionalities of tertiary and quaternary structural feature by modifying their primary sequences. Specific designs of leucine zippers promote the selective formation of coiled coils of two, three and four α-helices, with well-defined parallel or antiparallel orientation.[140-144] Employing such coiled coil structures on conducting surfaces provides a means for modifying the work function and the CTr properties of such interfaces. Helix coiled coil dimers provide three different configurations: (1) parallel orientation with N-termini attached to the metal and hence with the dipoles pointing away from the surface; (2) parallel orientation with C-termini attached to the metal and the dipoles pointing to the surface; and (3) antiparallel orientation where the oppositely pointing dipoles in each dimer cancel.[25] These three configurations results in three different sets of work functions of the conducting substrates. Junctions of these polypeptide surfaces, completed with conducting AFM tips, manifest CTr rectification and differences in their ohmic behavior.[25]

Despite the wealth of structural features that polypeptide offer, the limitations on the length of electron tunneling along their backbones presents a principal challenge for their use for CT systems. An alternative biopolymer, DNA, mediates efficient long-range CT via hole hopping, involving multiple ET steps.[35, 145] While the DNAs and RNAs are charge polymers, PNAs offer structural features for long-range hole hopping along the π-stacked bases, and the amides in the backbones provide an intrinsic macromolecular dipole.[36] While the dipoles of such single-stranded PNAs affects their CTr properties making them molecular electrets that can mediate long-range hole transfer and hole transport, the molecular dynamics of such single-strand polymers can have a prevalent effect on their CT capabilities. As an alternative, double-stranded PNAs have superior CT properties, even better than those of DNAs.[146] The PNA strands, however, have to be orientated in a parallel, rather than anti-parallel, manner. Otherwise, the dipoles of the two strands cancel out, similar to the coiled coil protein α-helices with antiparallel orientation.

The intrinsic dipole by bridging conjugates with the push-pull geometry provides an alternative for inducing rectification of CT and CTr. Using *para*-aminonitrophenylene derivatives as push-pull moieties encompasses a relatively straightforward strategy for introducing dipoles within CT pathways. Such dipolar phenylenes provide not only the dipoles, but also the electronic coupling along the CT pathways. The dipole affects the energy levels of the HOMOs and the LUMOs providing a cascade configuration for electrons to move downward toward the acceptor and the holes – upward toward the donor.[147] Incorporating such push-pull moieties in bridges, linking photosensitizers with semiconductor surfaces has the potential for controlling the kinetics of the interfacial PET, which has key implications for solar energy conversion applications. Considerations about the morphology and the surface chemistry of the semiconductor, and the relatively small dipoles of push-pull conjugates, present challenges for obtaining the desired CT kinetic behavior.[148-149]

The push-pull conjugates, cannot usually attain dipoles exceeding about 10 D over CT pathways distances of 1 nm or more.[115] Polypeptide α-helices and other macromolecular structures possess dipoles exceeding 30 D for an 1-nm stretch.[90] These electronic features demonstrate a key advantage that molecular electrets can offer. Indeed, molecular electrets composed of a sequence of push-pull moieties offers an attractive alternative.

6. Dipole effects in device design and engineering

Electronic devices comprising conjugated organic materials have a promising future as transistors[150], rectifiers[151], photodetectors[152] and organic light emitting diodes (OLEDs)[153]. In OLEDs, electrons and holes move from metal electrodes into organic materials where they recombine and emit light. Efficient electron injection is an important aspect of the process and one method of improving efficiency is to modify the Schottky energy barrier. Indeed, the smaller the barrier the more efficient the electron and hole injections. Modifying the electronic properties of materials interfaces proves immensely useful for design and development of devices.

In electronic devices, local fields originating from charge misbalance are intricate for materials interfaces. For organic and hybrid photovoltaics, for example, such interfacial fields may aid the photogenerated charge carrier to escape the Coulomb traps after the exciton dissociation.[154-156] Introducing molecular dipoles to surface designs provides a means for modifying the interfacial fields, i.e., enhance them, change their direction, or cancel them, depending on the targeted functionality.

Placing permanent dipole on surfaces of conductors and semiconductors changes their effective work functions. Anchoring dipolar molecules as SAMs to a metallic substrate further modifies its work function due to the formation of an interfacial dipole originating from: (1) the push-back of the metal electrons, reducing the intrinsic interfacial dipole, and (2) the charge redistribution resulting from the formation of bonds between the docking functional group and the metal surface. For example, the intrinsic dipoles of oligopeptides attached to gold nanoclusters change the reduction potentials of the oxidation of the metal particles.[157] When the dipoles point toward the gold surface they cause up to a 0.8-V positive shift in the reduction potentials.[157] Conversely, similar polypeptides attached to mercury surface cause negative shifts in the reduction potential of an axillary redox pair regardless the orientation of their dipoles.[158] This discrepancy indicates that other factors overcome the expected effects from the peptide dipoles.

Adsorption of ions presents a simpler manner for generating surface dipoles in comparison with forming SAMs of polar molecules. Such surface-charge electrets can impact significantly the performance of devices. Since the first reports by Grätzel *et al.*, dye-sensitized solar cells (DSSCs) have attracted considerable interest for their ability to convert solar light to electrical energy. In addition to the ruthenium-based photosensitizer, the initial designs employ lithium iodide as an electrolyte for the liquid junction and shuttling electrons from the cathode.[159] Since the first reports, it has become known that additives such as lithium ions and 4-*tert*-butylpyridine (TBP) affect the power-conversion efficiency of DSSCs.[160-161] It is commonly believed that the adsorption of Li^+ ions affects the band energies of TiO_2. Incorporation of the small positive ions into the surface of the TiO_2 lattice causes positive shift of the electrochemical potential of the semiconductor,[162] and increases the driving force for electron injection from the photoexcited sensitizer. Indeed, the diffusion coefficient and the undesired CR kinetics correlates with the Li^+ concentration.[163-164]

Evidences from transient absorption and electrochemical impedance spectroscopy suggest that improved electron injection efficiency is due to the interfacial dipole, pointing from the electrode to the electrolyte, originating from the lithium ions adsorbed on the titania nanocrystals, which in turn, facilitate exciton dissociation despite the small loss of photovoltage.[99, 165-166] In addition to affecting liquid-junction potentials, dipoles originated from adsorbed cations alter the properties of junctions between solid materials. Dynamics of ions, responsible for the interfacial dipoles and the energy-conversion efficiency of DSSCs and perovskite devices, causes the hysteresis at low frequencies.[167]

Surface dipoles from polar molecules attached to TiO_2 tunes the band-edge energies of the semiconductor and modulates the electron injection rates.[168] Incorporating permanent dipoles in CT conjugates, linking photosensitizers with the TiO_2 surface, is an important handle for improving the performance of DSSC. Three analogous porphyrin-bridge-anchor derivatives, two of which contain oppositely oriented intramolecular dipoles in the bridging unit, provide a means for examining this concept. Comparison between assemblies of these conjugates on the surface of mesoporous nanoparticle ZrO_2 films reveals *no* dipole effect on the electronic properties of the porphyrin.[148] The dipoles of the same conjugates attached to TiO_2 cause 200-meV shift in its bands energies. The dipole orientation, however, has no noticeable effect on the electron-injection rates. The relatively small magnitude of the dipoles in the bridging conjugates is most likely the reason for the lack of observable effect on the CT kinetics.[149]

Placing organic polar molecules, in an ordered manner, between two electrodes provides a means for controlling the *I-V* properties of the formed junctions. Molecular level rectification of the current is the most sought out property from such devices. These molecular or organic diodes mediate efficient CTr in one direction but not in the other, resulting in asymmetric *I-V* curves.

Metzger et al. utilize π-conjugated zwitterions as a CTr media for organic junctions.[100] Depositing monolayers or multilayers of such zwitterions between aluminum surfaces yields a junction that manifests superior rectifying *I-V* behavior.[100] Placing non-charged molecules with dipoles ranging from 2.8 to 6.8 D between gold surface and gold nanoparticles results in molecular junctions with a pronounced rectifying behavior. The ratios between the magnitude of the electric current against and along the dipole range between 2 and 9 for junctions comprising molecules with different dipole magnitude.[151, 169-170]

Ensuing, replacement of the groups for binding the polar molecules to the gold surfaces from thiol to isocyanide results in notable differences in rectification. This change in the anchoring groups causes more than two-fold reduction in the molecular dipole moment. Furthermore, calculations show a localization of the HOMO and LUMO on the terminal thiols, and delocalization of the frontier orbitals in the cyano-capped molecule.[171]

Assemblies of identical QDs with ligands with different dipoles, and thus different band energies, can generate cascades for directing electron and hole transport, e.g., "unidirectional" or "bidirectional" configuration for charge-transport pathways. Heterojunction PV devices, comprising such QD assemblies, show the favorability of the former, i.e., unidirectional configuration improves the power-conversion efficiency.[94] It is favorable because of a potential barrier for electrons or holes at the interface at different quantum dot layers.[94] The small size of the aromatic ligands ensures sufficient electronic coupling between neighboring QDs to ensure the efficiency of the interfacial charge transfer steps and of the long-range charge transport.

Coating silicon surfaces with small polar molecules with different dipole moments causes substantial effect on surface band bending and on the Si work function. Completing the "wiring" of the molecules with a metal electrode yields a junction with pronounced rectifying characteristics.[104] Such metal-semiconductor junction form Schottky diodes with

inherent dipole at the interface between the two materials. Intercalating polar organic SAMs between the metal and the semiconductor strongly affects the behavior of the Schottky diode. Metal-organic Schottky energy barriers follow ideal Schottky behavior. Namely, the electron Schottky barrier is determined by the energy difference between the metal work function and the electron affinity of the organic material, which is related to the reduction potential of the comprising molecules.[172] Thus, typically low work function metals are used for electron injection, and high work function metals – for hole injection.

Polar adsorbates allow for investigating the effects of a molecular dipole moment oriented both towards and away from an Ag electrode. These tests demonstrate control of the Schottky energy barrier. Specifically, when the dipole is oriented away from the electrode the energy barrier decreases; and when the dipole points toward the electrode the barrier increases.[173] The Schottky barrier height for an n-type semiconductor, ϕ_b, is estimated as:

$$\phi_b = \phi_m - \chi_{SC} + eV_i \qquad (8)$$

Where ϕ_m is the work function of the metal, χ_{SC} the electron affinity of the semiconductor, and V_i is the voltage drop due to an interface dipole which forms as a result of charge rearrangement upon the formation of the interface.[147] Cahen *et al.* report that molecular dipole monolayers as an effective tool for modifying barrier heights of Schottky junctions. The dipoles can affect both, ϕ_m and χ_{SC} of Au|SiO_2|Si diodes. Changing the terminal group from electron donating to electron withdrawing provides a means for altering the molecular dipole moment.[174-175]

Employing polar molecules in junctions for attaining CTr rectification presents two important challenges: (1) ensuring sufficient length of the organic CTr pathway between the two conducting or semiconducting electrodes; and (2) ensuring symmetry of the wiring of the

molecular species. Frequently, differences in the chemistry and the electronic properties of the manner of bonding of a molecule to the two electrodes may be the principal source of CTr rectification. Such asymmetry of the "wiring" to the electrodes can completely overcome any effect from the molecular dipoles.[112] When it comes to Schottky diodes, the semiconductor-metal junction is already asymmetric and the polar molecule only modify that asymmetry. Conversely, if the molecule is relatively small and strongly coupled electronically with the electrodes, the wave functions of the conducting substrate may penetrate through the whole molecule and perturb its electronic properties.[176] It may suppress the generated dipoles and eliminate the effects they may have.

Interfacing molecules with two electrodes presents some of the biggest challenges in the design of organic and molecular electronic devices. At the regions of molecular contacts, redistribution of the free charge carriers in the conducting substrates often generates fields that overwhelm the effects of the molecular dipoles in the junction. Molecular electrets that possess large dipoles and mediate long-range CT and CTr provide a means for eliminating the prevailing effect of the molecular contacts.

Conclusions

Field-induced changes in $-\Delta G_{ET}^{(0)}$ represent the principally accepted notion about the nature in which permanent dipoles affect CT. Synergies between the dipole effects on the Franck-Condon and electronic aspects of the CT kinetics illustrate some of the underlying complexity of this growing area of research. Donor-bridge-acceptor conjugates with permanent dipoles incorporated in their bridging moieties are excellent tools for expanding the basic understanding of the dependence of charge transfer on local electric fields. Placing similar dipolar conjugates between conducting and semiconducting electrodes, to form

electrical junctions, allows for bringing this basic knowledge to charge transport phenomena, setting the foundation for advanced molecular-level designs for electronic and energy-conversion applications.

Acknowledgements. We extend our gratitude to the USA National Science Foundation for their support (grant CHE 1465284), and for awarding a Graduate Research Fellowship to J.T. (GRFP grant DGE-1326120).

References

1. Rich, P. R.; Marechal, A., *Essays in Biochemistry* **2010,** *47* (Mitochondrial Function), 1. doi: 10.1042/bse0470001.
2. Gust, D.; Moore, T. A.; Moore, A. L., *Accounts of Chemical Research* **2009,** *42* (12), 1890. doi: 10.1021/ar900209b.
3. Kaerkaes, M. D.; Johnston, E. V.; Verho, O.; Aakermark, B., *Accounts of Chemical Research* **2014,** *47* (1), 100. doi: 10.1021/ar400076j.
4. Warren, J. J.; Winkler, J. R.; Gray, H. B., *Coordination Chemistry Reviews* **2013,** *257* (1), 165. doi: 10.1016/j.ccr.2012.07.002.
5. Fukuzumi, S.; Ohkubo, K.; Suenobu, T., *Accounts of Chemical Research* **2014,** *47* (5), 1455. doi: 10.1021/ar400200u.
6. Steffen, M. A.; Lao, K. Q.; Boxer, S. G., *Science* **1994,** *264* (5160), 810.
7. Tanaka, S.; Marcus, R. A., *Journal of Physical Chemistry B* **1997,** *101* (25), 5031.
8. Kamran, M.; Friebe, V. M.; Delgado, J. D.; Aartsma, T. J.; Frese, R. N.; Jones, M. R., *Nat Commun* **2015,** *6*.
9. Suydam, I. T.; Snow, C. D.; Pande, V. S.; Boxer, S. G., *Science* **2006,** *313* (5784), 200.

10. Sigala, P. A.; Fafarman, A. T.; Bogard, P. E.; Boxer, S. G.; Herschlag, D., *Journal of the American Chemical Society* **2007,** *129* (40), 12104.
11. Fried, S. D.; Bagchi, S.; Boxer, S. G., *Science* **2014,** *346* (6216), 1510.
12. Fried, S. D.; Boxer, S. G., *Science* **2015,** *349* (6251).
13. Sessler, G. M., *Top Appl Phys* **1987,** *33*, 13.
14. Sessler, G. M., *Top Appl Phys* **1987,** *33*, 1.
15. Xia, B.; Bao, D.; Upadhyayula, S.; Jones, G.; Vullev, V. I., *J. Org. Chem.* **2013,** *78* (5), 1994. doi: 10.1021/jo301942g.
16. Ashraf, M. K.; Pandey, R. R.; Lake, R. K.; Millare, B.; Gerasimenko, A. A.; Bao, D.; Vullev, V. I., *Biotechnology Progress* **2009,** *25* (4), 915.
17. Marcus, R. A., *Discuss Faraday Soc* **1960,** (29), 21. doi: 10.1039/DF9602900021.
18. Yomosa, S., *Sup Prog Theor Phys* **1967,** (40), 249.
19. Boxer, S. G., *Annu Rev Biophys Bio* **1990,** *19*, 267.
20. Galoppini, E.; Fox, M. A., *J. Am. Chem. Soc.* **1996,** *118* (9), 2299.
21. Fox, M. A.; Galoppini, E., *J. Am. Chem. Soc.* **1997,** *119* (23), 5277.
22. Knorr, A.; Galoppini, E.; Fox, M. A., *J Phys Org Chem* **1997,** *10* (7), 484.
23. Yasutomi, S.; Morita, T.; Imanishi, Y.; Kimura, S., *Science* **2004,** *304* (5679), 1944.
24. Gao, J. A.; Muller, P.; Wang, M.; Eckhardt, S.; Lauz, M.; Fromm, K. M.; Giese, B., *Angew Chem Int Edit* **2011,** *50* (8), 1926. doi: Doi 10.1002/Anie.201003389.
25. Shlizerman, C.; Atanassov, A.; Berkovich, I.; Ashkenasy, G.; Ashkenasy, N., *J. Am. Chem. Soc.* **2010,** *132* (14), 5070. doi: 10.1021/ja907902h.
26. Kapetanaki, S. M.; Ramsey, M.; Gindt, Y. M.; Schelvis, J. P. M., *Journal of the American Chemical Society* **2004,** *126* (20), 6214.
27. Sek, S.; Misicka, A.; Swiatek, K.; Maicka, E., *J Phys Chem B* **2006,** *110* (39), 19671. doi: Doi 10.1021/Jp063073z.

28. Sek, S.; Swiatek, K.; Misicka, A., *J Phys Chem B* **2005,** *109* (49), 23121. doi: Doi 10.1021/Jp055709c.

29. Winkler, J. R.; Di Bilio, A. J.; Farrow, N. A.; Richards, J. H.; Gray, H. B., *Pure and Applied Chemistry* **1999,** *71* (9), 1753.

30. Gray, H. B.; Winkler, J. R., *Quarterly Reviews of Biophysics* **2003,** *36* (3), 341.

31. Gray, H. B.; Winkler, J. R., *Proceedings of the National Academy of Sciences of the United States of America* **2005,** *102* (10), 3534.

32. Vullev, V. I.; Jones, G., II, *Research on Chemical Intermediates* **2002,** *28* (7-9), 795.

33. Venkatramani, R.; Keinan, S.; Balaeff, A.; Beratan, D. N., *Coordination Chemistry Reviews* **2011,** *255* (7-8), 635. doi: 10.1016/j.ccr.2010.12.010.

34. Lewis, F. D.; Zhu, H.; Daublain, P.; Fiebig, T.; Raytchev, M.; Wang, Q.; Shafirovich, V., *J. Am. Chem. Soc.* **2006,** *128* (3), 791. doi: 10.1021/ja0540831.

35. Lewis, F. D., *Israel Journal of Chemistry* **2013,** *53* (6-7), 350. doi: 10.1002/ijch.201300035.

36. Wolak, M. A.; Balaeff, A.; Gutmann, S.; Helmrich, H. J.; Vosloo, R.; Beerbom, M. M.; Wierzbinski, E.; Waldeck, D. H.; Bezer, S.; Achim, C.; Beratan, D. N.; Schlaf, R., *J. Phys. Chem. C* **2011,** *115* (34), 17123. doi: 10.1021/jp201602j.

37. Hamuro, Y.; Geib, S. J.; Hamilton, A. D., *Journal of the American Chemical Society* **1996,** *118* (32), 7529.

38. Vullev, V. I., *Journal of Physical Chemistry Letters* **2011,** *2* (5), 503.

39. Bahmani, B.; Guerrero, Y.; Bacon, D.; Kundra, V.; Vullev, V. I.; Anvari, B., *Laser Surg Med* **2014,** *46* (7), 582. doi: Doi 10.1002/Lsm.22269.

40. Bahmani, B.; Gupta, S.; Upadhyayula, S.; Vullev, V. I.; Anvari, B., *Journal of Biomedical Optics* **2011,** *16* (5), 051303/1. doi: 10.1117/1.3574761.

41. Bahmani, B.; Lytle, C. Y.; Walker, A. M.; Gupta, S.; Vullev, V. I.; Anvari, B., *Int. J. Nanomedicine* **2013,** *8*, 1609.

42. Mac, J. T.; Nuñez, V.; Burns, J. M.; Guerrero, Y. A.; Vullev, V. I.; Anvari, B., *Biomed. Opt. Express* **2016,** *7* (4), 1311. doi: 10.1364/BOE.7.001311.

43. Upadhyayula, S.; Quinata, T.; Bishop, S.; Gupta, S.; Johnson, N. R.; Bahmani, B.; Bozhilov, K.; Stubbs, J.; Jreij, P.; Nallagatla, P.; Vullev, V. I., *Langmuir* **2012,** *28* (11), 5059. doi: 10.1021/la300545v.

44. Gupta, S.; Chatni, M. R.; Rao, A. L. N.; Vullev, V. I.; Wang, L. V.; Anvari, B., *Nanoscale* **2013,** *5* (5), 1772. doi: 10.1039/c3nr34124k.

45. Guerrero, Y. A.; Bahmani, B.; Singh, S. P.; Vullev, V. I.; Kundra, V.; Anvari, B., *Nanotechnology* **2015,** *26* (43), 435102 (pp. 1. doi: 10.1088/0957-4484/26/43/435102.

46. Hammes-Schiffer, S., *J Am Chem Soc* **2015,** *137* (28), 8860. doi: 10.1021/jacs.5b04087.

47. Lennox, J. C.; Kurtz, D. A.; Huang, T.; Dempsey, J. L., *ACS Energy Letters* **2017**, Ahead of Print. doi: 10.1021/acsenergylett.7b00063.

48. Wierzchowski, J., *Nucleosides, Nucleotides & Nucleic Acids* **2014,** *33* (9), 626. doi: 10.1080/15257770.2014.913065.

49. Skonieczny, K.; Yoo, J.; Larsen, J. M.; Espinoza, E. M.; Barbasiewicz, M.; Vullev, V. I.; Lee, C.-H.; Gryko, D. T., *Chemistry - A European Journal* **2016,** *22*, 7485. doi: 10.1002/chem.201504944.

50. Trasatti, S., *Pure Appl Chem* **1986,** *58* (7), 955.

51. Latimer, W. M., *J Am Chem Soc* **1954,** *76* (4), 1200.

52. Rehm, D.; Weller, A., *Israel Journal of Chemistry* **1970,** *8* (2), 259.

53. Bao, D.; Millare, B.; Xia, W.; Steyer, B. G.; Gerasimenko, A. A.; Ferreira, A.; Contreras, A.; Vullev, V. I., *Journal of Physical Chemistry A* **2009,** *113* (7), 1259.

54. Born, M., *Zeitschrift fuer Physik* **1920,** *1*, 45.

55. Wan, J.; Ferreira, A.; Xia, W.; Chow, C. H.; Takechi, K.; Kamat, P. V.; Jones, G.; Vullev, V. I., *Journal of Photochemistry and Photobiology, A: Chemistry* **2008,** *197* (2-3), 364.

56. Bao, D.; Ramu, S.; Contreras, A.; Upadhyayula, S.; Vasquez, J. M.; Beran, G.; Vullev, V. I., *Journal of Physical Chemistry B* **2010,** *114* (45), 14467.

57. Marcus, R. A.; Sutin, N., *Biochim Biophys Acta* **1985,** *811* (3), 265.

58. Marcus, R. A., *Angew Chem Int Edit* **1993,** *32* (8), 1111.

59. Hush, N. S.; Vlcek, A. A.; Stranks, D. R.; Marcus, R. A.; Weiss, J.; Bell, R. P.; Halpern, J.; Orgel, L. E.; Adamson, A. W.; Dainton, F. S.; Williams, R. J. P.; Taube, H.; Shimi, I. A. W.; Higginson, W. C. E.; Stead, J. B.; Waind, G. M.; Rosseinsky, D. R.; Wells, C. F.; Sutcliffe, L. H.; Proll, P. J.; King, E. L.; Stranks, D. R.; Pearson, R. G.; Basolo, F.; Poe, A. J.; Fordsmith, M. H.; Sutin, N.; Dodson, R. W.; Baughan, C., *Discuss Faraday Soc* **1960,** (29), 113.

60. Yonemoto, E. H.; Riley, R. L.; Kim, Y. I.; Atherton, S. J.; Schmehl, R. H.; Mallouk, T. E., *Journal of the American Chemical Society* **1992,** *114* (21), 8081.

61. Bao, D.; Upadhyayula, S.; Larsen, J. M.; Xia, B.; Georgieva, B.; Nunez, V.; Espinoza, E. M.; Hartman, J. D.; Wurch, M.; Chang, A.; Lin, C.-K.; Larkin, J.; Vasquez, K.; Beran, G. J. O.; Vullev, V. I., *Journal of the American Chemical Society* **2014,** *136* (37), 12966. doi: 10.1021/ja505618n.

62. Jortner, J., *J Chem Phys* **1976,** *64* (12), 4860. doi: Doi 10.1063/1.432142.

63. Barbara, P. F.; Meyer, T. J.; Ratner, M. A., *J Phys Chem-Us* **1996,** *100* (31), 13148. doi: Doi 10.1021/Jp9605663.

64. Marcus, R. A., *J Electroanal Chem* **2000,** *483* (1-2), 2. doi: Doi 10.1016/S0022-0728(00)00011-5.

65. Upadhyayula, S.; Bao, D.; Millare, B.; Sylvia, S. S.; Habib, K. M. M.; Ashraf, K.; Ferreira, A.; Bishop, S.; Bonderer, R.; Baqai, S.; Jing, X.; Penchev, M.; Ozkan, M.; Ozkan, C. S.; Lake, R. K.; Vullev, V. I., *Journal of Physical Chemistry B* **2011,** *115* (30), 9473. doi: 10.1021/jp2045383.

66. Yonemoto, E. H.; Saupe, G. B.; Schmehl, R. H.; Hubig, S. M.; Riley, R. L.; Iverson, B. L.; Mallouk, T. E., *Journal of the American Chemical Society* **1994,** *116* (11), 4786.

67. Clark, C. D.; Debad, J. D.; Yonemoto, E. H.; Mallouk, T. E.; Bard, A. J., *Journal of the American Chemical Society* **1997,** *119* (43), 10525.

68. Savoie, B. M.; Rao, A.; Bakulin, A. A.; Gelinas, S.; Movaghar, B.; Friend, R. H.; Marks, T. J.; Ratner, M. A., *Journal of the American Chemical Society* **2014,** *136* (7), 2876.

69. Savoie, B. M.; Jackson, N. E.; Chen, L. X.; Marks, T. J.; Ratner, M. A., *Accounts of Chemical Research* **2014,** *47* (11), 3385.

70. Heitzer, H. M.; Savoie, B. M.; Marks, T. J.; Ratner, M. A., *Angewandte Chemie-International Edition* **2014,** *53* (29), 7456.

71. Hu, J.; Xia, B.; Bao, D.; Ferreira, A.; Wan, J.; Jones, G.; Vullev, V. I., *Journal of Physical Chemistry A* **2009,** *113* (13), 3096.

72. Miller, J. R.; Calcaterra, L. T.; Closs, G. L., *Journal of the American Chemical Society* **1984,** *106* (10), 3047.

73. Miller, J. R.; Beitz, J. V.; Huddleston, R. K., *Journal of the American Chemical Society* **1984,** *106* (18), 5057.

74. Closs, G. L.; Miller, J. R., *Science* **1988,** *240* (4851), 440.

75. Kakitani, T.; Mataga, N., *Journal of Physical Chemistry* **1985,** *89* (1), 8.

76. Onsager, L., *Journal of the American Chemical Society* **1936,** *58*, 1486.

77. Mataga, N.; Kaifu, Y.; Koizumi, M., *B Chem Soc Jpn* **1956,** *29* (4), 465.

78. Lippert, E., *Zeitschrift fuer Naturforschung* **1955,** *10a*, 541.

79. Ooshika, Y., *J Phys Soc Jpn* **1954,** *9* (4), 594.

80. Pina, J.; de Melo, J. S.; Breusov, D.; Scherf, U., *Physical Chemistry Chemical Physics* **2013,** *15* (36), 15204.

81. Palsson, L. O.; Wang, C. S.; Batsanov, A. S.; King, S. M.; Beeby, A.; Monkman, A. P.; Bryce, M. R., *Chem-Eur J* **2010,** *16* (5), 1470.

82. Dejaegere, A.; Karplus, M., *Journal of Physical Chemistry* **1996,** *100* (26), 11148.

83. Doyle, D. A.; Cabral, J. M.; Pfuetzner, R. A.; Kuo, A. L.; Gulbis, J. M.; Cohen, S. L.; Chait, B. T.; MacKinnon, R., *Science* **1998,** *280* (5360), 69. doi: Doi 10.1126/Science.280.5360.69.

84. Dutzler, R.; Campbell, E. B.; Cadene, M.; Chait, B. T.; MacKinnon, R., *Nature* **2002,** *415* (6869), 287. doi: Doi 10.1038/415287a.

85. Simmons, J. G., *J Appl Phys* **1963,** *34* (6), 1793.

86. Stark, J., *Nature* **1913,** *92*, 401.

87. Stark, J., *Annalen der Physik (Berlin, Germany)* **1914,** *43*, 965.

88. Bublitz, G. U.; Boxer, S. G., *Annu Rev Phys Chem* **1997,** *48*, 213.

89. Hovick, J. W.; Poler, J. C., *J Chem Educ* **2005,** *82* (6), 889.

90. Shin, Y.-G. K.; Newton, M. D.; Isied, S. S., *J Am Chem Soc* **2003,** *125* (13), 3722.

91. Voller, J.-S.; Budisa, N.; Biava, H.; Hildebrandt, P., *Biochimica et biophysica acta* **2017**.

92. Fried, S. D.; Boxer, S. G., *Accounts of Chemical Research* **2015,** *48* (4), 998. doi: 10.1021/ar500464j.

93. Albero, J.; Martinez-Ferrero, E.; Iacopino, D.; Vidal-Ferran, A.; Palomares, E., *Physical Chemistry Chemical Physics* **2010,** *12* (40), 13047.

94. Santra, P. K.; Palmstrom, A. F.; Tanskanen, J. T.; Yang, N.; Bent, S. F., *Journal of Physical Chemistry C* **2015,** *119* (6), 2996. doi: 10.1021/acs.jpcc.5b00341.

95. Jones, G., II; Yan, D.; Hu, J.; Wan, J.; Xia, B.; Vullev, V. I., *Journal of Physical Chemistry B* **2007,** *111* (24), 6921.

96. Purc, A.; Espinoza, E. M.; Nazir, R.; Romero, J. J.; Skonieczny, K.; Jezewski, A.; Larsen, J. M.; Gryko, D. T.; Vullev, V. I., *Journal of the American Chemical Society* **2016,** *138* (39), 12826. doi: 10.1021/jacs.6b04974.

97. Vasquez, J. M.; Vu, A.; Schultz, J. S.; Vullev, V. I., *Biotechnology Progress* **2009,** *25* (4), 906.

98. Jones, G., II; Lu, L. N.; Vullev, V.; Gosztola, D.; Greenfield, S.; Wasielewski, M., *Bioorganic & Medicinal Chemistry Letters* **1995,** *5* (20), 2385.

99. Bai, Y.; Zhang, J.; Wang, Y. H.; Zhang, M.; Wang, P., *Langmuir* **2011,** *27* (8), 4749. doi: 10.1021/la200156m.

100. Metzger, R. M.; Chen, B.; Hopfner, U.; Lakshmikantham, M. V.; Vuillaume, D.; Kawai, T.; Wu, X. L.; Tachibana, H.; Hughes, T. V.; Sakurai, H.; Baldwin, J. W.; Hosch, C.; Cava, M. P.; Brehmer, L.; Ashwell, G. J., *J Am Chem Soc* **1997,** *119* (43), 10455. doi: Doi 10.1021/Ja971811e.

101. Hol, W. G. J., *Advances in Biophysics* **1985,** *19*, 133.

102. Hol, W. G. J.; Van Duijnen, P. T.; Berendsen, H. J. C., *Nature* **1978,** *273* (5662), 443.

103. Wada, A., *Journal of Chemical Physics* **1959,** *30*, 328.

104. Hiremath, R. K.; Rabinal, M. K.; Mulimani, B. G.; Khazi, I. M., *Langmuir* **2008,** *24* (19), 11300. doi: 10.1021/la800882e.

105. Hunger, R.; Jaegermann, W.; Merson, A.; Shapira, Y.; Pettenkofer, C.; Rappich, J., *Journal of Physical Chemistry B* **2006,** *110* (31), 15432.

106. Alloway, D. M.; Hofmann, M.; Smith, D. L.; Gruhn, N. E.; Graham, A. L.; Colorado, R.; Wysocki, V. H.; Lee, T. R.; Lee, P. A.; Armstrong, N. R., *Journal of Physical Chemistry B* **2003,** *107* (42), 11690.

107. Frey, S.; Shaporenko, A.; Zharnikov, M.; Harder, P.; Allara, D. L., *Journal of Physical Chemistry B* **2003,** *107* (31), 7716.

108. Zenasni, O.; Marquez, M. D.; Jamison, A. C.; Lee, H. J.; Czader, A.; Lee, T. R., *Chem Mater* **2015,** *27* (21), 7433.

109. Ballav, N.; Schupbach, B.; Neppl, S.; Feulner, P.; Terfort, A.; Zharnikov, M., *Journal of Physical Chemistry C* **2010,** *114* (29), 12719.

110. Meyerbroker, N.; Zharnikov, M., *Langmuir* **2012,** *28* (25), 9583.

111. Abu-Husein, T.; Schuster, S.; Egger, D. A.; Kind, M.; Santowski, T.; Wiesner, A.; Chiechi, R.; Zojer, E.; Terfort, A.; Zharnikov, M., *Adv Funct Mater* **2015,** *25* (25), 3943.

112. Jia, C. C.; Guo, X. F., *Chem Soc Rev* **2013,** *42* (13), 5642.

113. Anne, F. B.; Purpan, F. D.; Jacquemin, D., *Chemical Physics Letters* **2013,** *581*, 52. doi: 10.1016/j.cplett.2013.07.021.

114. Akemann, W.; Laage, D.; Plaza, P.; Martin, M. M.; Blanchard-Desce, M., *Journal of Physical Chemistry B* **2008,** *112* (2), 358. doi: 10.1021/jp075418z.

115. Bures, F., *Rsc Adv* **2014,** *4* (102), 58826.

116. Takashima, S.; Asami, K., *Biopolymers* **1993,** *33* (1), 59. doi: 10.1002/bip.360330107.

117. Kimura, S., *Organic & Biomolecular Chemistry* **2008,** *6* (7), 1143. doi: 10.1039/b717898k.

118. Kuemin, M.; Schweizer, S.; Ochsenfeld, C.; Wennemers, H., *Journal of the American Chemical Society* **2009,** *131* (42), 15474.

119. Wierzbinski, E.; de Leon, A.; Yin, X.; Balaeff, A.; Davis, K. L.; Reppireddy, S.; Venkatramani, R.; Keinan, S.; Ly, D. H.; Madrid, M.; Beratan, D. N.; Achim, C.; Waldeck, D. H., *Journal of the American Chemical Society* **2012,** *134* (22), 9335.

120. Larsen, J. M.; Espinoza, E. M.; Hartman, J. D.; Lin, C.-K.; Wurch, M.; Maheshwari, P.; Kaushal, R. K.; Marsella, M. J.; Beran, G. J. O.; Vullev, V. I., *Pure Appl. Chem.* **2015,** *87* (8), 779. doi: 10.1515/pac-2015-0109.

121. Larsen, J. M.; Espinoza, E. M.; Vullev, V. I., *J. Photon. Energy.* **2015,** *5* (1), 055598 (pp. 1. doi: 10.1117/1.JPE.5.055598.

122. Espinoza, E. M.; Larsen, J. M.; Vullev, V. I., *Journal of Physical Chemistry Letters* **2016,** *7* (5), 758. doi: 10.1021/acs.jpclett.5b02881.

123. Larsen-Clinton, J. M.; Espinoza, E. M.; Mayther, M. F.; Clark, J.; Tao, C.; Bao, D.; Larino, C. M.; Wurch, M.; Lara, S.; Vullev, V. I., *Physical Chemistry Chemical Physics* **2017,** *19* (11), 7871. doi: 10.1039/c7cp00432j.

124. Espinoza, E. M.; Larsen, J. M.; Vullev, V. I., *ECS Transactions* **2015,** *66* (23), 1.

125. Espinoza, E. M.; Larsen-Clinton, J. M.; Krzeszewski, M.; Darabedian, N.; T., G. D.; Vullev, V. I., *Pure Appl. Chem.* **2017**, ahead of print. doi: 10.1515/pac-2017-0309.

126. Espinoza, E. M.; Vullev Valentine, I., *ECS Transactions* **2017,** *77*, 1517.

127. Fedorova, A.; Chaudhari, A.; Ogawa, M. Y., *J Am Chem Soc* **2003,** *125* (2), 357. doi: 10.1021/ja026140l.

128. Beratan, D. N.; Onuchic, J. N.; Winkler, J. R.; Gray, H. B., *Science* **1992,** *258* (5089), 1740.

129. Jones, G., II; Vullev, V. I., *Organic Letters* **2002,** *4* (23), 4001.

130. Jones, G., II; Zhou, X.; Vullev, V. I., *Photochemical & Photobiological Sciences* **2003,** *2* (11), 1080.

131. Garbuio, L.; Antonello, S.; Guryanov, I.; Li, Y.; Ruzzi, M.; Turro, N. J.; Maran, F., *J. Am. Chem. Soc.* **2012,** *134* (25), 10628. doi: 10.1021/ja303696s.

132. Cordes, M.; Kottgen, A.; Jasper, C.; Jacques, O.; Boudebous, H.; Giese, B., *Angewandte Chemie-International Edition* **2008,** *47* (18), 3461.

133. Giese, B.; Wang, M.; Gao, J.; Stoltz, M.; Muller, P.; Graber, M., *J Org Chem* **2009,** *74* (10), 3621. doi: Doi 10.1021/Jo900375f.

134. Kitagawa, K.; Morita, T.; Kimura, S., *Langmuir* **2005,** *21* (23), 10624. doi: 10.1021/la050776j.

135. Okamoto, S.; Morita, T.; Kimura, S., *Langmuir* **2009,** *25* (5), 3297. doi: 10.1021/la8034962.

136. Boncheva, M.; Vogel, H., *Biophys J* **1997,** *73* (2), 1056.

137. Arikuma, Y.; Nakayama, H.; Morita, T.; Kimura, S., *Angewandte Chemie, International Edition* **2010,** *49* (10), 1800. doi: 10.1002/anie.200905621.

138. Mandal, H. S.; Kraatz, H. B., *Chem Phys* **2006,** *326* (1), 246. doi: Doi 10.1016/J.Chemphys.2006.01.010.

139. Odonnell, J. F.; Mann, C. K., *J Electroanal Chem* **1967,** *13* (1-2), 157.

140. Harbury, P. B.; Zhang, T.; Kim, P. S.; Alber, T., *Science* **1993,** *262* (5138), 1401.

141. Jones, G., II; Vullev, V.; Braswell, E. H.; Zhu, D., *Journal of the American Chemical Society* **2000,** *122* (2), 388.

142. Jones, G., II; Vullev, V. I., *Organic Letters* **2001,** *3* (16), 2457.

143. Vullev, V. I.; Jones, G., *Tetrahedron Letters* **2002,** *43* (47), 8611.

144. Jones, G., II; Vullev, V. I., *Journal of Physical Chemistry A* **2001,** *105* (26), 6402.

145. Kawai, K.; Majima, T., *Accounts of Chemical Research* **2013,** *46* (11), 2616. doi: 10.1021/ar400079s.

146. Beratan, D. N.; Liu, C.; Migliore, A.; Polizzi, N. F.; Skourtis, S. S.; Zhang, P.; Zhang, Y., *Accounts of Chemical Research* **2015,** *48* (2), 474. doi: 10.1021/ar500271d.

147. Ishii, H.; Sugiyama, K.; Ito, E.; Seki, K., *Advanced Materials* **1999,** *11* (8), 605. doi: 10.1002/(sici)1521-4095(199906)11:8<605::aid-adma605>3.0.co;2-q.

148. Ngo, K. T.; Rochford, J.; Fan, H.; Batarseh, A.; Chitre, K.; Rangan, S.; Bartynski, R. A.; Galoppini, E., *Faraday Discussions* **2015,** *185*, 497. doi: 10.1039/c5fd00082c.

149. Nieto-Pescador, J.; Abraham, B.; Li, J. J.; Batarseh, A.; Bartynski, R. A.; Galoppini, E.; Gundlach, L., *Journal of Physical Chemistry C* **2016,** *120* (1), 48. doi: 10.1021/acs.jpcc.5b09463.

150. Sekitani, T.; Zschieschang, U.; Klauk, H.; Someya, T., *Nature Materials* **2010,** *9* (12), 1015. doi: 10.1038/nmat2896.

151. Morales, G. M.; Jiang, P.; Yuan, S. W.; Lee, Y. G.; Sanchez, A.; You, W.; Yu, L. P., *Journal of the American Chemical Society* **2005,** *127* (30), 10456. doi: 10.1021/ja051332c.

152. Zhang, H.; Jenatsch, S.; De Jonghe, J.; Nuesch, F.; Steim, R.; Veron, A. C.; Hany, R., *Scientific Reports* **2015,** *5*. doi: 10.1038/srep09439.

153. Ly, K. T.; Chen-Cheng, R. W.; Lin, H. W.; Shiau, Y. J.; Liu, S. H.; Chou, P. T.; Tsao, C. S.; Huang, Y. C.; Chi, Y., *Nature Photonics* **2017,** *11* (1), 63. doi: 10.1038/nphoton.2016.230.

154. Zhu, X. Y.; Yang, Q.; Muntwiler, M., *Accounts of Chemical Research* **2009,** *42* (11), 1779. doi: 10.1021/ar800269u.

155. Barbour, L. W.; Hegadorn, M.; Asbury, J. B., *J Am Chem Soc* **2007,** *129* (51), 15884.

156. Lu, H.; Bao, D.; Penchev, M.; Ghazinejad, M.; Vullev, V. I.; Ozkan, C. S.; Ozkan, M., *Advanced Science Letters* **2010,** *3* (2), 101.

157. Holm, A. H.; Ceccato, M.; Donkers, R. L.; Fabris, L.; Pace, G.; Maran, F., *Langmuir* **2006,** *22* (25), 10584. doi: 10.1021/la061553b.

158. Becucci, L.; Guryanov, I.; Maran, F.; Guidelli, R., *Journal of the American Chemical Society* **2010,** *132* (17), 6194. doi: 10.1021/ja100486y.

159. Oregan, B.; Gratzel, M., *Nature* **1991,** *353* (6346), 737. doi: 10.1038/353737a0.

160. Katoh, R.; Kasuya, M.; Kodate, S.; Furube, A.; Fuke, N.; Koide, N., *Journal of Physical Chemistry C* **2009,** *113* (48), 20738. doi: 10.1021/jp906190a.

161. Koops, S. E.; O'Regan, B. C.; Barnes, P. R. F.; Durrant, J. R., *Journal of the American Chemical Society* **2009,** *131* (13), 4808. doi: 10.1021/ja8091278.

162. Kelly, C. A.; Farzad, F.; Thompson, D. W.; Stipkala, J. M.; Meyer, G. J., *Langmuir* **1999,** *15* (20), 7047. doi: 10.1021/la990617y.

163. Kambe, S.; Nakade, S.; Kitamura, T.; Wada, Y.; Yanagida, S., *Journal of Physical Chemistry B* **2002,** *106* (11), 2967. doi: 10.1021/jp013397h.

164. Haque, S. A.; Tachibana, Y.; Willis, R. L.; Moser, J. E.; Gratzel, M.; Klug, D. R.; Durrant, J. R., *Journal of Physical Chemistry B* **2000,** *104* (3), 538. doi: 10.1021/jp991085x.

165. Yu, Q. J.; Wang, Y. H.; Yi, Z. H.; Zu, N. N.; Zhang, J.; Zhang, M.; Wang, P., *Acs Nano* **2010,** *4* (10), 6032. doi: 10.1021/nn101384e.

166. Jennings, J. R.; Wang, Q., *Journal of Physical Chemistry C* **2010,** *114* (3), 1715. doi: 10.1021/jp9104129.

167. Contreras, L.; Idigoras, J.; Todinova, A.; Salado, M.; Kazim, S.; Ahmad, S.; Anta, J. A., *Physical Chemistry Chemical Physics* **2016,** *18* (45), 31033. doi: 10.1039/c6cp05851e.

168. Meng, S.; Kaxiras, E., *Nano Letters* **2010,** *10* (4), 1238. doi: 10.1021/nl100442e.

169. Jiang, P.; Morales, G. M.; You, W.; Yu, L. P., *Angewandte Chemie-International Edition* **2004,** *43* (34), 4471. doi: 10.1002/anie.200460110.

170. Oleynik, II; Kozhushner, M. A.; Posvyanskii, V. S.; Yu, L., *Physical Review Letters* **2006,** *96* (9). doi: 10.1103/PhysRevLett.96.096803.

171. Lee, Y. G.; Carsten, B.; Yu, L., *Langmuir* **2009,** *25* (3), 1495. doi: 10.1021/la802923a.

172. Parker, I. D., *Journal of Applied Physics* **1994,** *75* (3), 1656. doi: 10.1063/1.356350.

173. Campbell, I. H.; Rubin, S.; Zawodzinski, T. A.; Kress, J. D.; Martin, R. L.; Smith, D. L.; Barashkov, N. N.; Ferraris, J. P., *Physical Review B* **1996,** *54* (20), 14321.

174. Vilan, A.; Shanzer, A.; Cahen, D., *Nature* **2000,** *404* (6774), 166.

175. Selzer, Y.; Cahen, D., *Advanced Materials* **2001,** *13* (7), 508. doi: 10.1002/1521-4095(200104)13:7<508::aid-adma508>3.0.co;2-8.

176. Sayed, S. Y.; Fereiro, J. A.; Yan, H. J.; McCreery, R. L.; Bergren, A. J., *Proceedings of the National Academy of Sciences of the United States of America* **2012,** *109* (29), 11498. doi: Doi 10.1073/Pnas.1201557109.

Figure Captions

Figure 1. Bioinspired molecular electrets based on anthranilamide (Aa) motifs. (a) Origin of the ground-state electric macrodipole dipole of Aa electrets from ordered orientation of the amide linkers and from the polarization due to the formation of the hydrogen bonds. (b) Long-range charge transduction mediated via electron hopping, or on-resonance electron transport, along the Aa residues and the effect of the macrodipole on the preferred directionality of the ET steps.

Figure 2. Molecular orbital (MO) diagrams representing long-range photoinduced charge transfer occurring via different mechanisms, involving photoexcitation, **1**, followed by a sequence of discrete electron-transfer step, **2** to **5**. The transferred electrons are encircled.

Figure 3. Band-MO diagrams showing charge transport through a metal-molecule-metal junction occurring via different mechanisms that are governed by the alignment between the Fermi energies of the electrodes, E_f, and the energy levels of the frontier molecular orbitals. The transferred electrons on the HOMOs are encircled.

Figure 4. Electric dipole moment and its ordered co-directional assemblies to illustrate the origin of the macrodipoles in electerts. Vector sums of dipoles from stacked and head-to-tail arrangements lead to the same total dipole moment (eq. 7).

Figure 5. MO diagrams showing the dipole effects on long-range PET occurring via different mechanisms, mediated by D-B-A conjugates. (a,b) For tunneling, or superexchange mechanism, the photoexcitation, **1**, is followed by a long-range electron-tunneling step, **2**.

The electret dipole alters the energy levels of the frontier orbitals, and most importantly, the reduction potentials of the donor and the acceptor. Therefore, $\Delta G_{ET}^{(0)}$ is different for ET along and against the dipole. (c) For electron hopping along the dipole, the photoexcitation, **1**, is followed by multiple short tunneling steps, i.e., hopping steps, **2** to **5**. The electret dipole alters the energy levels of the frontier orbitals generating cascade ET pathways along the bridge, i.e., each hopping step has $\Delta G_{ET}^{(0)} < 0$, which is immensely beneficial for long range ET. In comparison, in the absence of a dipole, each hopping step has $\Delta G_{ET}^{(0)} = 0$ (Figure 2c). (d) For electron hopping against the dipole, the photoexcitation, **1**, is followed by a hopping step, **2**, and a long-range tunneling step, **3**. The number of hopping steps for this case depends on the extent to which the dipole field shifts the energy levels of the frontier orbitals. The diagrams do not show CR steps that will be especially prevalent when ET is against the dipole for hopping mechanism (c), where CR will efficiently compete with step **3**.

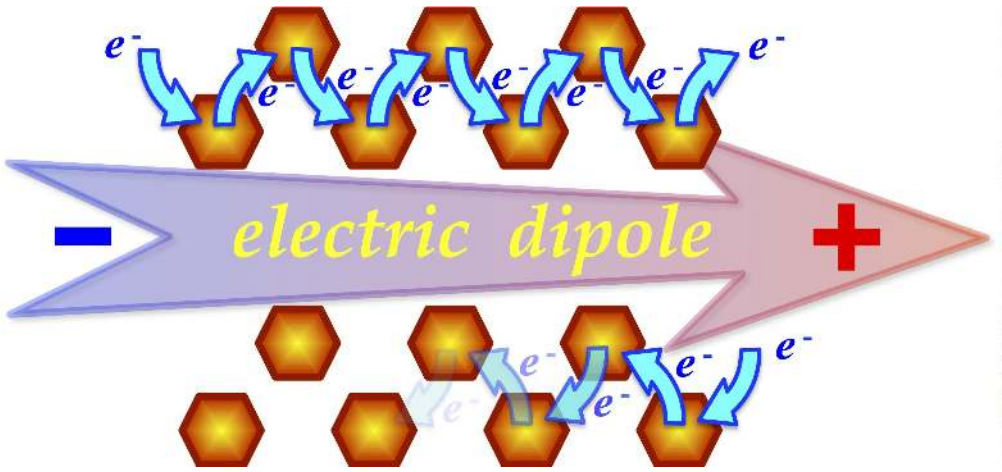

190x88mm (300 x 300 DPI)

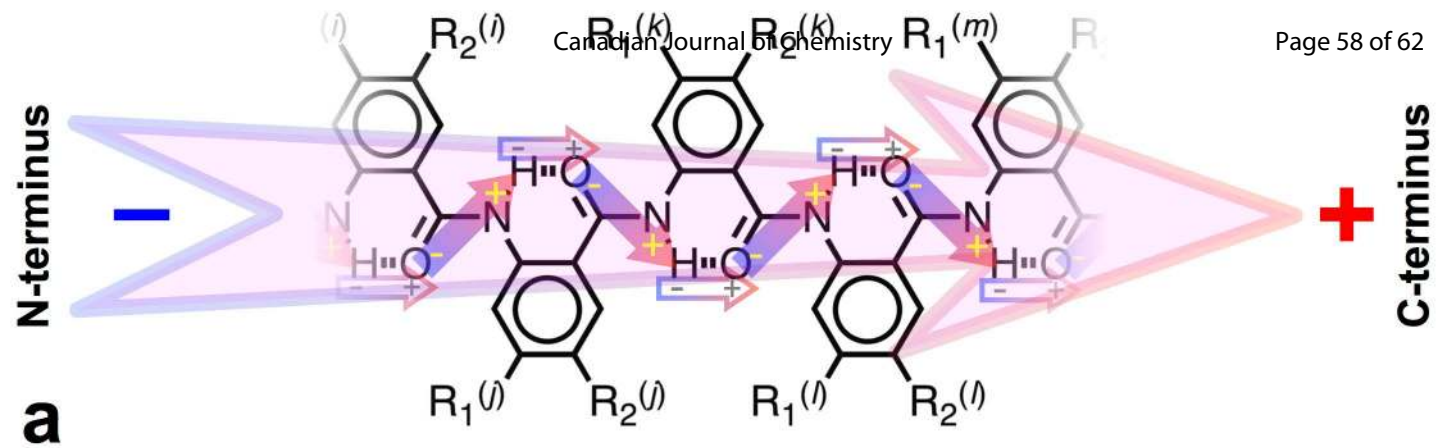
N-terminus
C-terminus
a

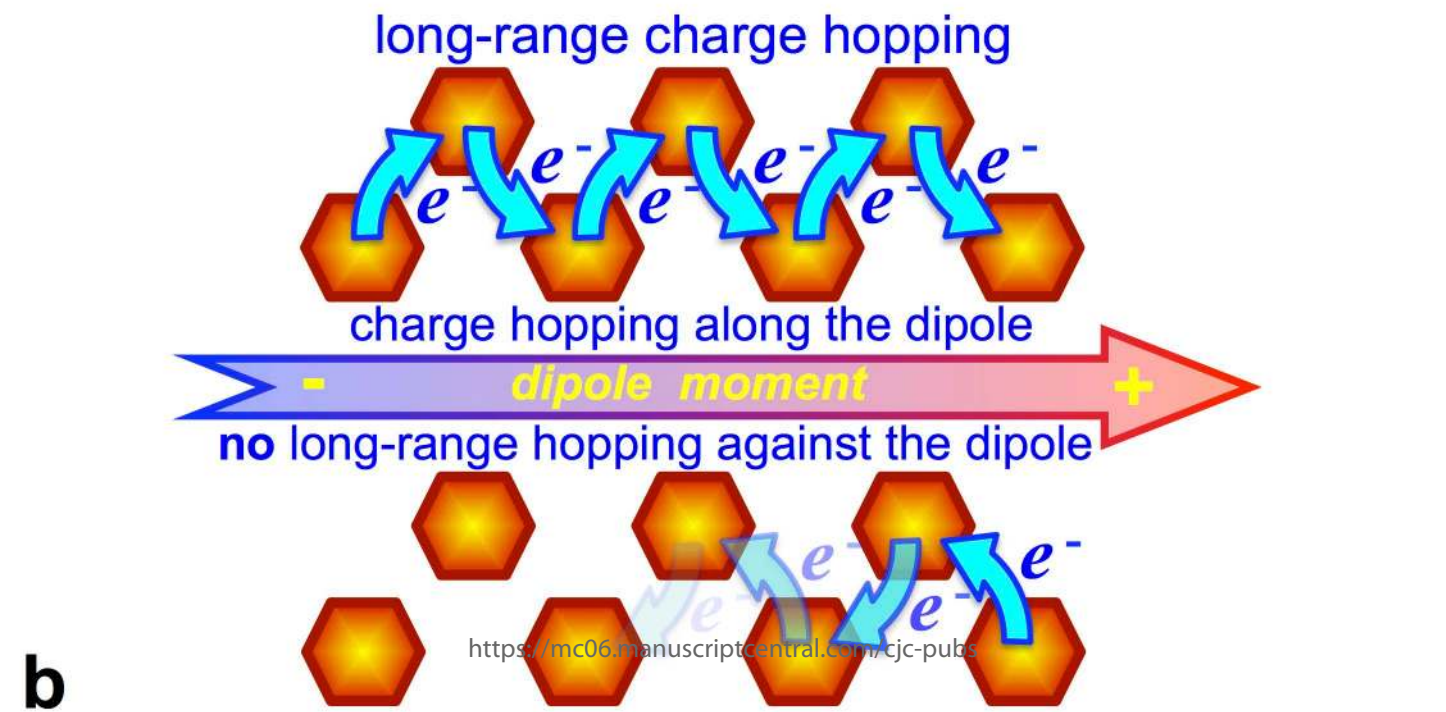
long-range charge hopping
charge hopping along the dipole
dipole moment
no long-range hopping against the dipole
b

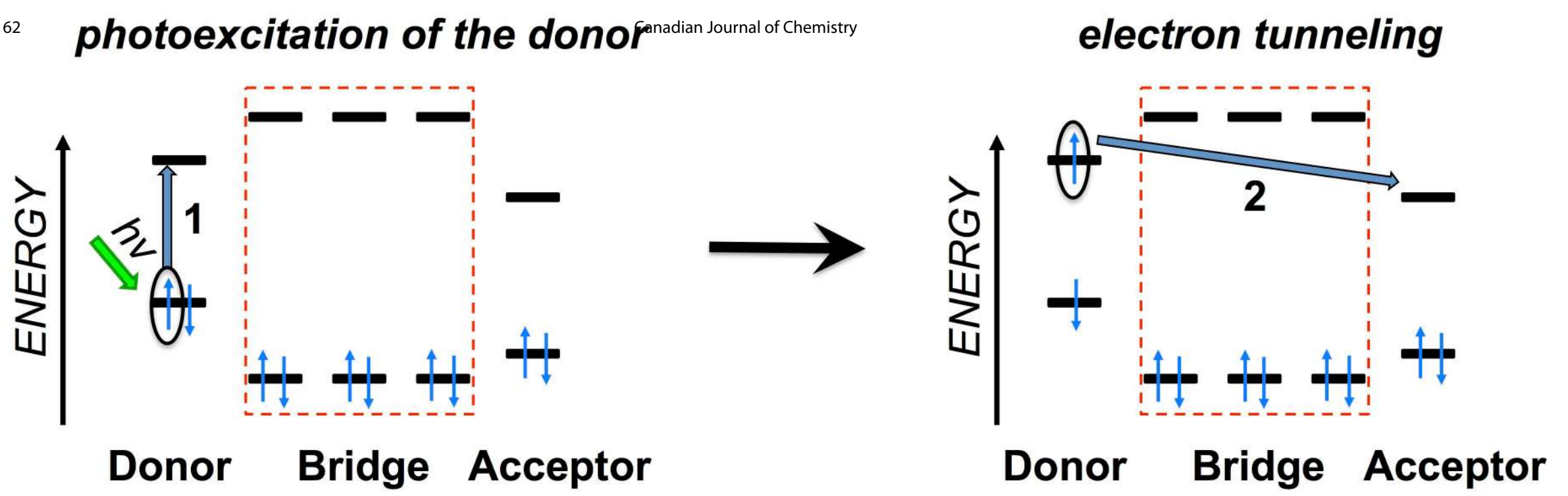
photoexcitation of the donor
electron tunneling
ENERGY
hν
1
2
Donor
Bridge
Acceptor
a
photoexcitation of the acceptor
hole tunneling
ENERGY
1
hν
2
Donor
Bridge
Acceptor
b
photoexcitation of the donor
electron hopping
ENERGY
hν
1
2
3
4
5
Donor
Bridge
Acceptor
c
photoexcitation of the acceptor
hole hopping
ENERGY
1
hν
5
4
3
2
Donor
Bridge
Acceptor
d

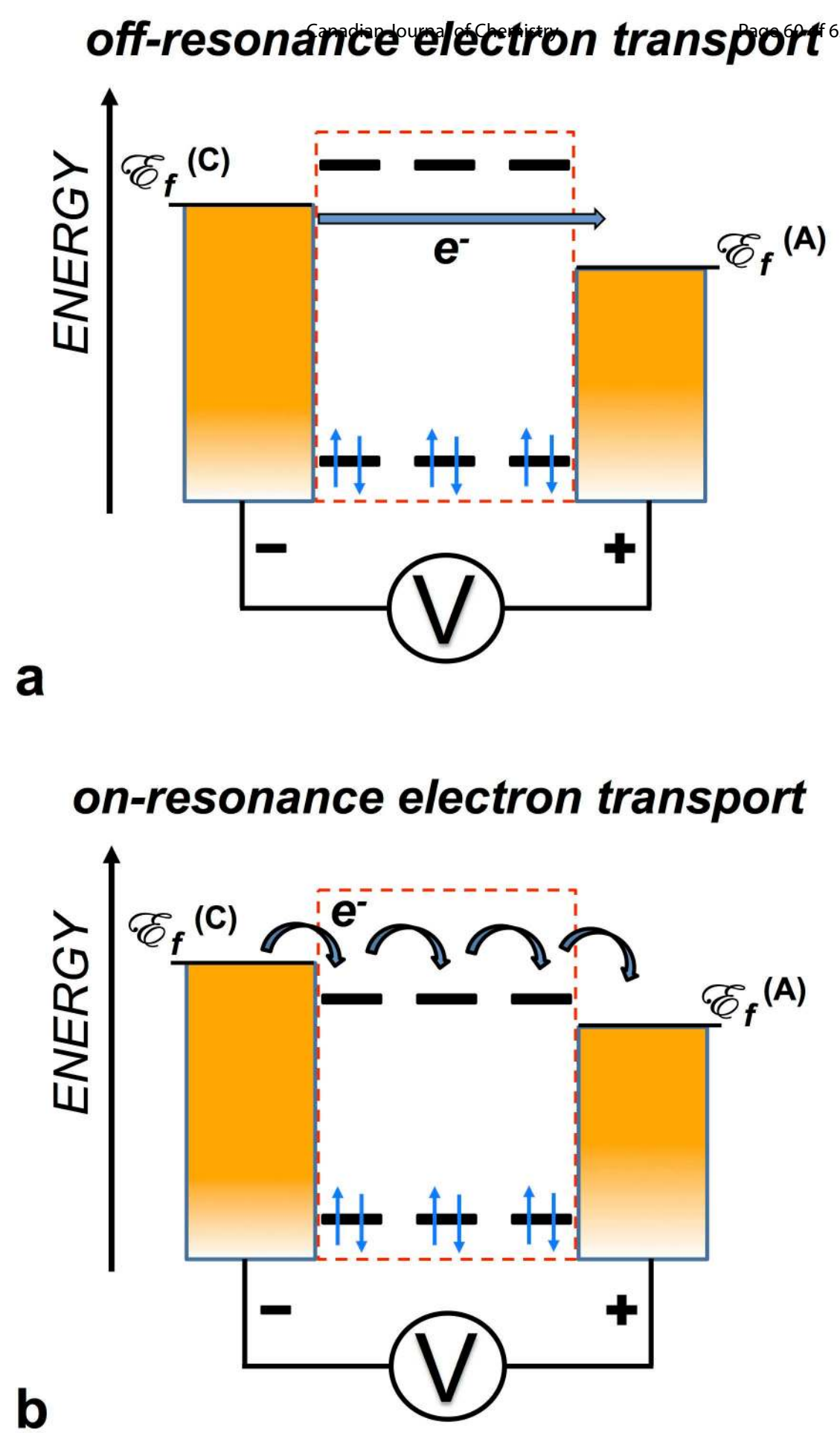
off-resonance electron transport
ENERGY
$\mathscr{E}_f$ (C)
e-
$\mathscr{E}_f$ (A)
-
+
V

a

on-resonance electron transport
ENERGY
$\mathscr{E}_f$ (C)
e-
$\mathscr{E}_f$ (A)
-
+
V

b

on-resonance hole transport
ENERGY
$\mathscr{E}_f$ (C)
e-
$\mathscr{E}_f$ (A)
-
+
V

c

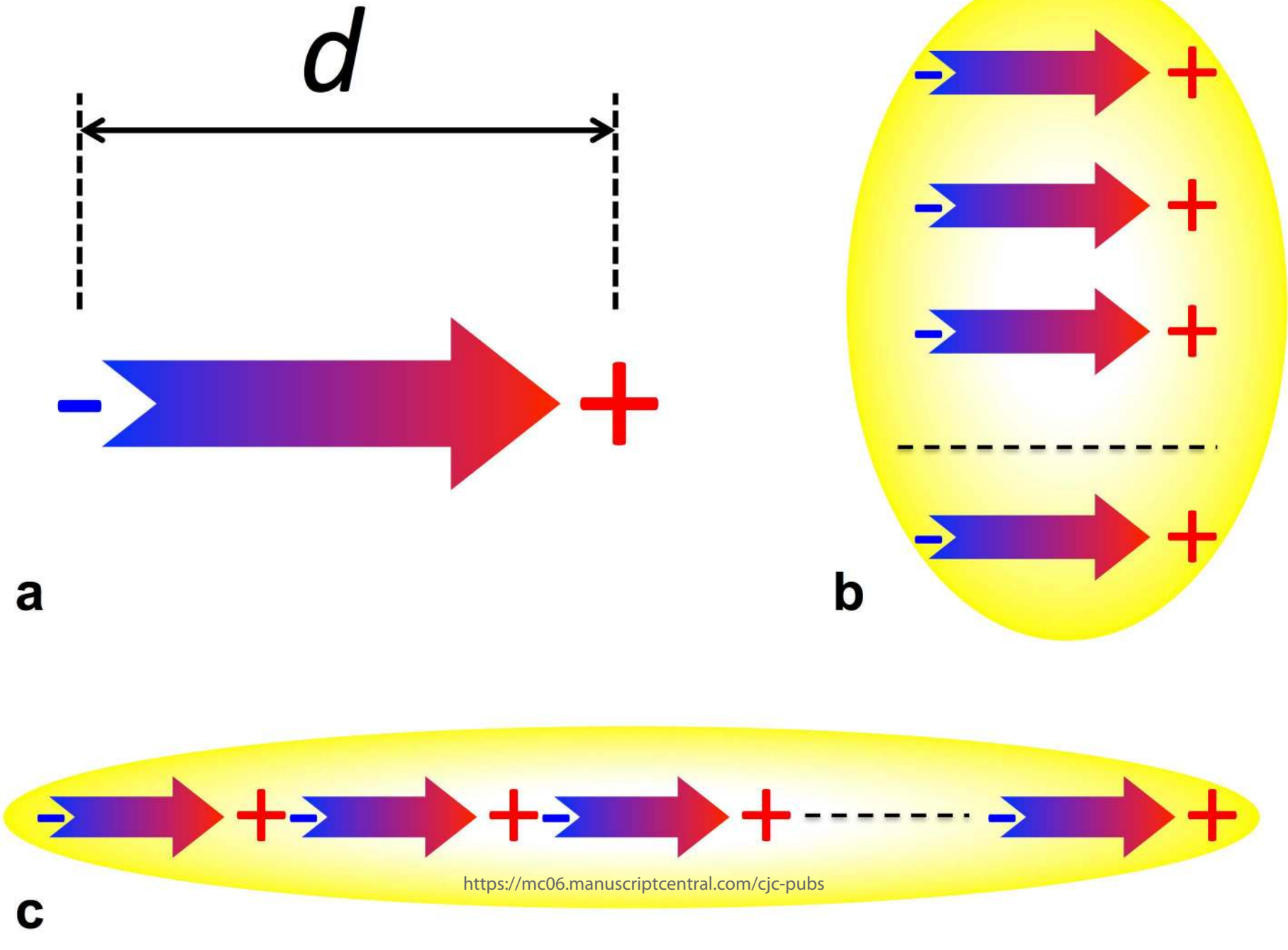
d
a
b
c

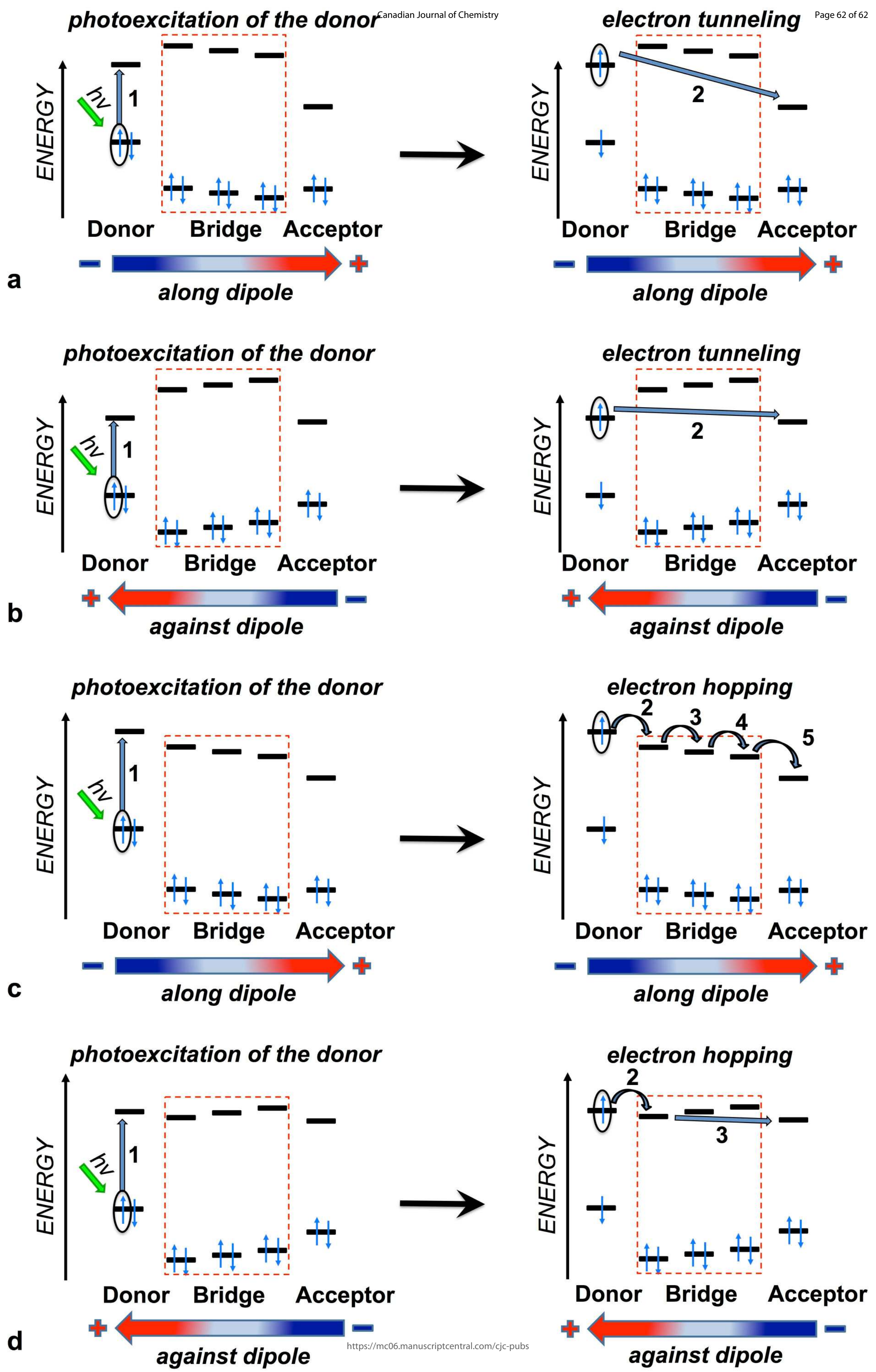
photoexcitation of the donor
electron tunneling
ENERGY
hν
1
2
Donor
Bridge
Acceptor
along dipole
against dipole
electron hopping
3
4
5
a
b
c
d